



**HAL**  
open science

## Mechanochemical cleavage of wheat lignin into a more homogeneous fraction

Nadja Cachet, Pierre Lavedan, Michel Baltas, Bouchra Benjelloun-Mlayah

► **To cite this version:**

Nadja Cachet, Pierre Lavedan, Michel Baltas, Bouchra Benjelloun-Mlayah. Mechanochemical cleavage of wheat lignin into a more homogeneous fraction. *Industrial Crops and Products*, 2024, 221, pp.119321. 10.1016/j.indcrop.2024.119321 . hal-04693246

**HAL Id: hal-04693246**

**<https://hal.science/hal-04693246v1>**

Submitted on 11 Sep 2024

**HAL** is a multi-disciplinary open access archive for the deposit and dissemination of scientific research documents, whether they are published or not. The documents may come from teaching and research institutions in France or abroad, or from public or private research centers.

L'archive ouverte pluridisciplinaire **HAL**, est destinée au dépôt et à la diffusion de documents scientifiques de niveau recherche, publiés ou non, émanant des établissements d'enseignement et de recherche français ou étrangers, des laboratoires publics ou privés.

1 **Mechanochemical cleavage of wheat lignin into a more homogeneous**  
2 **fraction**

3 Nadja Cachet<sup>1,3</sup>, Pierre Lavedan<sup>2</sup>, Michel Baltas<sup>3\*</sup>, Bouchra Benjelloun-Mlayah<sup>1\*</sup>

4

5 <sup>1</sup> CIMV, 109 rue Jean Bart, Diapason A, F-31670 Labège, France

6 <sup>2</sup> Institut de Chimie de Toulouse, UAR 2599, 118 Route de Narbonne, Toulouse Cedex  
7 09, 31062, France

8 <sup>3</sup> CNRS, LCC (Laboratoire de Chimie de Coordination), Université de Toulouse, UPS,  
9 205 Route de Narbonne, BP 44099, Cedex 4, 31077 Toulouse, France

10 \* Corresponding authors Email: michel.baltas@lcc-toulouse.fr; b.benjelloun@cimv.fr

11

12 **ABSTRACT**

13 Lignin, the second most abundant biopolymer in earth, represents nature's largest  
14 carbon sources, has high polydispersity and uncertain reactivity, that limit efficient  
15 modification/degradation and use of products obtained. In order to decrease by  
16 mechanochemical means the average molecular mass and polydispersity of lignin  
17 fragments of the CIMV organosolv lignin named Biolignin<sup>TM</sup>, we applied a sodium  
18 hydroxide-assisted planetary ball milling process. Experimental conditions were first  
19 optimized on purified Biolignin<sup>TM</sup> then to Biolignin<sup>TM</sup> without prior purification in 20ml  
20 jars before applying it successfully to a 500 ml planetary ball milling apparatus.  
21 Extensive, quantitative HSQC NMR, IR and GPC studies, overtaken supported our  
22 three most important findings: reduction of the needed quantity of sodium hydroxide of  
23 75% compared to the literature, obtention of halve (-51%) the occurrence of  $\beta$ -O-4'

24 linkages in lignin fragment, an optimum of 14 wt% of moisture is useful in the  
25 degradation process.

26 **Keywords:** organosolv lignin degradation, mechanical milling,  $\beta$ -O-4-linkages cleavage

27

## 28 **1. Introduction**

29 Lignin, the second most abundant biopolymer in earth after cellulose, represents  
30 nature's largest carbon sources with an annual production of about 20 billion tons. In  
31 contrast to cellulose and hemicellulose, lignin is highly branched heterogenous  
32 polyphenolic material, without a recurring structural unit in the biomass. In that respect,  
33 lignin has high polydispersity and consequently uncertain reactivity, two important  
34 factors that limit efficient modification/degradation and use of products obtained.  
35 Mechanical energy and mechanochemistry, besides the fact that allowed the  
36 development of sustainable and efficient chemical transformations by promoting the  
37 formation of new bonds and non-covalent interactions, has also demonstrated its  
38 potential in the selective cleavage of specific chemical bonds.

39 Lignins can be obtained by various methods resulting in different characteristics.

40 Technical lignins mainly gathered kraft, sulphite, soda-anthaquinone and organosolv  
41 lignins. Organosolv lignins are the most recent and promising ones. Organosolv  
42 processes are considered to be the most efficient and environmentally friendly way to  
43 extract lignin from biomass. It allows the obtention of lignin with a relatively lower  
44 molecular weight and more homogeneous fragments resulting a lower polydispersity  
45 compared to others technical lignins. However, even these more homogeneous lignins  
46 are still suitable for direct use to a limited extent.

47 The valorisation of lignins in the era of green and environmental preserved world,  
48 generated a tremendous activity in fundamental (and consequently industrial) research  
49 during the last two decades. The quest for lignin derived chemical platforms (low  
50 molecular mass compounds and essentially monomers), oriented important work on  
51 homogenous, heterogenous catalysis, use of alternative solvents, and thermochemical,  
52 oxidative, photocatalytic or biochemical depolymerization methods (Zhou *et al.* 2022  
53 and Sun *et al.* 2018 and references therein). Usually, each method is associated with its  
54 own benefits and drawbacks; it is also important to point out that each kind of lignin is  
55 unique (purity, dispersity, molecular weight...) so each method should be adapted to the  
56 lignin studied. Oxidative depolymerization of lignin is one of the most studied aspects  
57 (Abdelaziz *et al.* 2022).

58 Some ten years ago, mechanochemistry entered in the field of lignin degradation. In  
59 2013, Kleine *et al.* reported a pioneering work on the lignin depolymerization *via*  
60 mechanochemical grinding and in the presence of solid bases (Kleine *et al.* 2013).  
61 Mechanochemical oxidative processing is also reported since the last decade by many  
62 authors. As an example, the mechanochemical oxidation and cleavage of the  $\beta$ -O-4 in  
63 lignin systems has been reported in the presence of catalytic amounts of HO-  
64 TEMPO/KBr/Oxone, resulting in monomeric products efficiently in order to be applied  
65 in upscale batch reactions (Dabral *et al.* 2018). Very recently, a novel mechano-  
66 enzymatic strategy was developed (Xu *et al.* 2023) for lignin depolymerization leading  
67 into functional aromatic monomers considered as high value chemicals for  
68 pharmaceutical, material and energy industries.

69 Also, very recently, surface modification of a kraft lignin by grinding with sodium  
70 percarbonate and sodium hydroxide as an oxidant can lead to reduction in  
71 polydispersity and improved water adsorption (Fink *et al.* 2023).

72  
73 The aim of our study concerns a specific organosolv lignin named Biolignin™  
74 The objective of this work is to halve the average molecular weight lignin fragments of  
75 Biolignin™ without highly modifying its functional groups content in order to avoid  
76 any decrease of its reactivity and to enhance its ability to substitute phenol or polyols in  
77 various industrial applications.

78 Indeed, in some applications in which Biolignin™ was used as the substitute of  
79 petrochemical molecules (phenol, PEG) (Tachon *et al.*, 2016; Llovera *et al.*, 2016), the  
80 limiting factor of the substitution might be the molecular mass of lignin fragments.

81 Lignin fragments are not totally linear and reactive groups such as phenolic and  
82 aliphatic OH, could be sterically shielded, affecting the global reactivity of lignin.

83 Decreasing the length of lignin fragment might enhance the accessibility of such  
84 functional groups for further coupling reactions.

## 85 **2. Materials and methods**

### 86 *2.1.Extraction and solvent fractionation of the organosolv lignin*

87 The organosolv lignin studied below is named Biolignin™. Biolignin™ was extracted  
88 at pilot scale from wheat straw at the CIMV pilot plant (Compiègne, France). The  
89 CIMV organosolv process consists in a fractionation of lignocellulosic materials thanks  
90 to a mixture of acetic acid/formic acid/water (55:30:15, w/w/w) during 3.5 hours at  
91 105°C and at atmospheric pressure. The lignin is separated from the extraction liquor by  
92 adding water to the concentrated liquor to induce its precipitation. It is finally recovered

93 by filtrating the above liquid suspension (Figure 1) (Benjelloun-Mlayah and Delmas  
94 2019).

95 **[Figure 1]**

96 In order to increase the lignin content (increase the purity) and to decrease the  
97 polydispersity of lignin fragments, the Biolignin<sup>TM</sup> was sequentially fractionated with  
98 diethyl ether (99.7% stabilized with ~6 ppm of BHT, PanReac), dichloromethane  
99 (99.8% stabilized with ~20 ppm of amylene, PanReac) and methanol (99.9% UV-IR-  
100 HPLC-GPC Grade, PanReac) as illustrated in Figure 2. This purification was previously  
101 developed by the CIMV research group in order to obtain a purified Biolignin<sup>TM</sup>, highly  
102 concentrated in similar lignin fragments and gathered nearly 50% (w/w) of  
103 unfractionated Biolignin<sup>TM</sup> (unpublished results).

104 Before fractionation, the Biolignin<sup>TM</sup> was dried at 50°C in a drying oven, until obtaining  
105 at least 96% of Dry Matter (DM). The dry Biolignin<sup>TM</sup> was then grounded in a ceramic  
106 mortar to enhance its contact surface.

107 **[Figure 2]**

108 An amount (100g) of dried and grounded Biolignin<sup>TM</sup> was introduced in a 2L-  
109 cylindrical reactor equipped of a frit n°3 (pore size: 16-40 µm). Then, 500 mL of the  
110 respective solvent was added and the mixture was mechanically stirred during 1 hour at  
111 room temperature. After removing the solvent by pumping through the frit, 500 mL of  
112 the identical fresh solvent was added and the mixture stirred during 1 hour. This  
113 procedure was repeated several times until the majority of the soluble molecules seemed  
114 to be eluted (final filtrate nearly colorless). The next solvent was then added to the  
115 remaining Biolignin<sup>TM</sup> sample and the same procedure was applied.

116 All the filtrates of each solvent were combined and evaporated under reduced pressure  
117 to obtain the three global fractions: F1 (6.4%  $\pm$ 0.5 w/w), F2 (16.2%  $\pm$ 1.2 w/w) and  
118 Purified Biolignin<sup>TM</sup> (48.4%  $\pm$ 2.2 w/w). The insoluble residue (29.0%  $\pm$ 2.7 w/w) was  
119 composed of the remaining solid residue after methanol elution. F1 was recovered as a  
120 brown-yellow sticky residue, F2 as brown-yellow flakes and Purified Biolignin<sup>TM</sup> as  
121 sparkled black flakes.

122

## 123 2.2. *Biolignin<sup>TM</sup> content analyses*

### 124 2.2.1. *Ash content*

125 Ash content was determined by the combustion of 1g of accurately weighted sample  
126 (accuracy:  $10^{-4}$ ) with a known moisture content. The sample was placed in an oven at  
127 600°C during 24h. The weight of ash remaining was calculated as a percentage of the  
128 original dry weight of sample. At least two measurements were done on each sample.

129

### 130 2.2.2. *Elemental analysis and proteins content*

131 Elemental analyses were performed on a PerkinElmer 2400 Series II CHNS/O  
132 Elemental Analyzer. 2.0 mg ( $\pm$  0.5mg) of sample were weighed. Only C, H and N  
133 elements were analyzed. The proteins content was deduced from the % of N using the  
134 nitrogen-to-protein conversion factor (5.4 for wheat straw, Marriotti *et al.* 2008). At  
135 least two measurements were done on each sample.

136

### 137 2.2.3. *Cellulose and hemicellulose content in lignin*

138 Residual cellulose and hemicellulose contents of lignin fractions were determined based  
139 on NREL method (Sluiter *et al.* 2008): The glucose and xylose contained in the fraction

140 were quantified by HPLC, after chemical hydrolysis. The hydrolysis was conducted in 2  
141 steps: 0.2 g of dry lignin sample was powdered in 1.6 ml of H<sub>2</sub>SO<sub>4</sub> 72% (12 M) and  
142 stirred at room temperature overnight, followed by stirring at 30°C for 1 hour. For the  
143 second step, 22.4 g of distilled water was added and the mixture was maintained at  
144 120°C for 1 hour.  
145 Then, the samples were cooled at room temperature before their analysis by HPLC for  
146 sugars quantification. The following HPLC conditions were used: Eluent: H<sub>2</sub>SO<sub>4</sub> 0.005  
147 M; Flow rate: 0.6 ml/min; Column Hi-Plex H column (300 x 7.7 mm), temperature  
148 80°C; Detector Refractometer, temperature 50°C. At least two measurements were done  
149 on each sample.

150

#### 151 *2.2.4. Infrared spectroscopic analyses*

152 Infrared analyses were conducted with an attenuated total reflectance system (ATR) on  
153 a PerkinElmer Spectrum 100 Universal ATR-FTIR instrument equipped with a  
154 diamond/ZnSe crystal single reflection. 10 mg of dried sample were placed on the  
155 crystal plate on which a constant pressure of 85 N/mm<sup>2</sup> was applied. Each spectrum was  
156 obtained after 8 scans at a resolution of 4 cm<sup>-1</sup>. At least two measurements were done on  
157 each sample.

158

#### 159 *2.2.5. Gel Permeation Chromatography (GPC)*

160 The molecular-average weights of samples were determined by Gel Permeation  
161 Chromatography (GPC). GPC analyses were carried out on a Water 1515 Isocratic  
162 HPLC Pump equipped with a Water 2414 Refractive Index Detector. Three stainless  
163 steel columns (Phenomenex, Phenogel. 300 x 7.8 mm. 5 µm) connected in series and



164 packed with a styrene-divinylbenzene copolymer of porosity 100, 500 and  $10^3$  Å,  
165 respectively, were used. The following operating conditions were employed: Eluent,  
166 THF (Panreac, UV-IR-HPLC-GPC Grade); temperature, 38°C; sample concentration,  
167 5 mg/mL; injection volume, 20 µL; flow rate, 0.8 mL/min. Polystyrene (PS) standards  
168 used for the GPC calibration curve have a molecular weight of: 4910, 3180, 2590, 2170,  
169 1530, 990, 770, 580 and 380 Da. The standards concentration in THF was set at  
170 2 mg/mL.

171 The samples were injected without prior derivatization. To limit the presence of  
172 insoluble particles in the injected samples, they were previously dissolved in a mixture  
173 of 1,4-Dioxane/Methanol (1:1, v/v), (Panreac, UV-IR-HPLC Grade) to reach a  
174 concentration of 40 mg/mL. When necessary (samples degraded by NaOH), the samples  
175 were neutralized by addition of hydrochloric acid in an amount equivalent to the sodium  
176 hydroxide. The solution was then diluted with THF (HPLC Grade) to obtain a final  
177 concentration of 10 mg/mL. The solution was then filtrated through a 0.45 µm  
178 membrane before analysis. At least two measurements were done on each sample. The  
179 molecular weight of lignin was quantified relative to polystyrene standards and was  
180 therefore not absolute.  $M_n$  represent the number average Molecular weight,  $M_w$ , the  
181 weight average molecular weight and I the polydispersity index of the polymer  
182 ( $I=M_w/M_n$ ).

183

#### 184 2.2.6. *Quantitative $^{31}P$ NMR*

185 Hydroxyl groups and aromatic carboxylic acids of lignin samples were quantified by  
186  $^{31}P$ -NMR. Each sample was phosphitylated with 2-Chloro-4,4,5,5-tetramethyl-1,3,2-  
187 dioxaphospholane (95%, Sigma Aldrich, St. Louis, MO, USA). For these experiments,

188 endo-N-hydroxy-5-norbornene-2,3-dicarboximide (97%, Sigma Aldrich, St. Louis, MO,  
189 USA) was selected as the internal standard. The whole experimental procedure is  
190 described by Cachet and Benjelloun-Mlayah (2021). At least two measurements were  
191 done on each sample.

192

### 193 2.2.7. $^1\text{H}$ - $^{13}\text{C}$ 2D-NMR experiments

194 NMR experiments were performed at 25°C on a Bruker Advance 500 MHz  
195 spectrometer equipped with a 5 mm gradient cryoprobe with inverse geometry (5 mm  
196 CPTCI 1H-31P/13C Z-GRD Z44913/0001). 125 mg of each sample (without prior  
197 derivatization) were dissolved in 750  $\mu\text{L}$  of DMSO- $d_6$ . Chemical shifts ( $\delta$  in ppm) are  
198 referenced to the carbon ( $\delta_{\text{C}}$  39.53 ppm) and the residual proton ( $\delta_{\text{H}}$  2.50 ppm) signals of  
199 DMSO- $d_6$  (99.8%D, Eurisotop, Saint Aubin, France)

200 The two-dimensional heteronuclear single quantum coherence (HSQC) - NMR  
201 experiments were conducted using Bruker's "hsqcetgp" pulse with spectral widths of  
202 6002 Hz (from 11.5 to -0.50 ppm) and 22638 Hz (from 175 to -5 ppm) for the  $^1\text{H}$ - and  
203  $^{13}\text{C}$ - dimension, respectively. The number of collection complex points was 1024 for the  
204  $^1\text{H}$ - dimension with a recycle delay of 2 s. The number of transients was 16, and 1024  
205 times increments were always recorded in the  $^{13}\text{C}$ - dimension. The  $^1\text{J}_{\text{CH}}$  used was 145  
206 Hz. Processing used typical squared sine-bell apodization for the  $^1\text{H}$ - and  $^{13}\text{C}$ -  
207 dimension. Prior to Fourier transformation, the data matrixes were zero-filled up to  
208 1024 points in the  $^{13}\text{C}$ - dimension.

209 The semi-quantitative analysis of the volume integrals (uncorrected) of the HSQC  
210 correlation peaks was performed using MestRec 4.9.9.3 processing software. This

211 quantification was conducted following the procedure described by Wen *et al.* (2013)  
212 and by Sette *et al.* (2011).

213

### 214 2.3. Mechanochemical reactions

215 Mechanochemical reactions were mainly inspired by the work of Brittain *et al.* (2018).

216 Ball-milling of lignin was performed in two ZrO<sub>2</sub> jars (20 mL) in parallel, at room

217 temperature using a planetary Fritsch Pulverisette 7 Premium Line ball mill. The jars

218 were equipped with five milling balls each (10 mm diameter, ZrO<sub>2</sub>). The ball-milling

219 was carried out at 800 rpm for 15 to 120 min. To avoid overheating at long milling

220 times, the mill was stopped for 5 min after every 30 min of milling. The milling jars

221 were filled with crude or purified Biolignin<sup>TM</sup> and sodium hydroxide powder (97%,

222 Sigma Aldrich, St Louis, MO, USA). The quantity of solid products in each jar was set

223 at 700 to 1000 mg according to the experiment. Preliminary experiments confirmed that

224 no positive or negative effects were observed varying the quantity of solid products

225 from 700 mg to 1000 mg. The ratio of Biolignin<sup>TM</sup>/NaOH was adjusted from 1:1 (w/w)

226 to 4:1 (w/w) according to the experiment. The samples were left to sit for 5 min–24 h

227 before being prepared for molecular mass analysis in order to study the quenching effect

228 of the reaction. Each jar was analyzed separately by GPC in order to evaluate the

229 repeatability of the experiment. If the two results of a same experiment were too

230 different (*i.e.* >10%), the experiment was repeated twice. The values reported on this

231 study are the average of the values obtained in experiments under the same conditions.

232 Before analyses, the grinded samples were neutralized by solubilization in water (50

233 mg/mL) and slowly adding dropwise concentrated HCl (37%, Pharma Grade, PanReac)

234 in an amount equivalent to the sodium hydroxide used for the reaction. The pH value

235 was checked with pH test stripes (pH 1-14, ChemSolute) and adjusted if needed in order  
236 to precipitate lignin. The medium was centrifuged (4000 RPM, 2x 15 min). The solid  
237 lignin was then separated to the aqueous phase and washed 3 times with UHQ H<sub>2</sub>O by  
238 filtration on a frit n°3 (pore size: 16-40 μm). The final solid was dried at 50°C in a  
239 drying oven during 24 hours.

240 Some experiments were assisted by a small amount of liquid in order to enhance the  
241 reactivity of the depolymerization. The amount of liquid was set in order to respect the  
242 conditions of Liquid-assisted grinding (LAG) empirically defined by the parameter  $\eta$   
243 [ $\eta = V(\text{liquid}; \mu\text{L}) / m(\text{solid reagents}; \text{mg})$ ]. LAG conditions are operating when values  
244 of  $\eta$  range 0–2 μL/mg, the reaction appears independent of reactant solubility (Ying *et*  
245 *al.* 2021).

246 For ion scavenging tests, methanol (0.27μL/mg of Biolignin<sup>TM</sup>,  $\eta$  0.22) was added to the  
247 lignin/sodium hydroxide mixture in the milling jar. To investigate the influence of the  
248 moisture content, water was added to the milling jar to increase the total moisture  
249 content in the sample from its original value of 4 wt% to the desired moisture content.

250 A control experiment was made milling *ca.* 700 mg of purified Biolignin<sup>TM</sup> without  
251 sodium hydroxide powder (97%, Sigma Aldrich, St Louis, MO, USA) in a 20 mL ZrO<sub>2</sub>  
252 jar with five milling balls (10 mm diameter, ZrO<sub>2</sub>) during 120 min, with a 5 min stop  
253 every 30 minutes to cool down the system.

254 To test the scale up of the reaction, ball-milling of lignin was performed in a Tungsten  
255 Carbide (WC) jar (500 mL) using a Retsch PM 100 ball mill at room temperature. The  
256 jar was equipped with 10 or 20 milling balls according to the experiment (20 mm  
257 diameter, WC). The ball-milling was carried out at 650 rpm for 60 minutes. To avoid  
258 overheating at long milling times, the mill was stopped for 10 min after every 15 min of

259 milling. The milling jar was filled with Biolignin<sup>TM</sup> and sodium hydroxide powder. The  
260 quantity of products was set at 21.0g ± 0.5g. The ratio of Biolignin<sup>TM</sup>/Sodium  
261 hydroxide was set at an equimolar ratio between C9-Unit (162g/ mol) and NaOH. The  
262 influence of the moisture content was made by adding water to the milling jar to  
263 increase the total moisture content in the sample from its original value of 4 wt% to the  
264 desired moisture content.

265

### 266 **3. Results and discussion**

#### 267 *3.1. Extraction and fractionation of lignin from wheat straw*

268 The mechanochemistry is a method of choice to obtain valuable products in a green  
269 way. Thus, the more environmentally friendly production of organosolv lignins among  
270 technical lignins, leads us to select this kind of lignin. Moreover, organosolv lignins are  
271 composed of relatively homogeneous lignin fragments. Indeed, less energy will be  
272 required to obtain more homogeneous fragments with a low average molecular weight  
273 than if another technical lignin is used.

274 To obtain the organosolv lignin studied below, the wheat straw was treated at  
275 atmospheric pressure with a mixture of organic acids (acetic acid and formic acid) and  
276 water at 105°C during 3.5 hours (Benjelloun-Mlayah and Delmas 2019). These  
277 conditions allowed the dissolution of lignin fragments and hemicelluloses in the acidic  
278 media. After filtration to remove the solid part (cellulose fraction), the lignin was  
279 precipitated and separated from the extraction liquor. The precipitated fraction mainly  
280 composed of lignin, is named Biolignin<sup>TM</sup> and represents 27% (w/w, Dry Matter) of the  
281 initial wheat straw.

282 The Biolignin<sup>TM</sup> was not entirely composed of lignin fragments. Some constituents of  
283 wheat straw, like ashes, residual carbohydrates and proteins, were also precipitated with

284 lignin fragments during its separation from the extraction liquor. Table 1 summarized  
285 and quantified these constituents (see experimental sections 2.2.1 to 2.2.3).

286 **[Table 1]**

287 As, showed in Table 2, lignin fragments of Biolignin<sup>TM</sup> had restricted distribution  
288 ( $M_w/M_n < 2$ ). However, this distribution and the impurities contained in the Biolignin<sup>TM</sup>  
289 fraction (Table 1) could have a negative influence for depolymerization/degradation of  
290 lignin fragment by mechanochemistry. In literature, most of the time, the  
291 depolymerization of lignin is optimized using synthetic lignin models (dimers or  
292 trimers) before testing on natural lignin (Dabral *et al.* 2018, Sun *et al.* 2020, Xu *et al.*  
293 2023). For the study below, a direct use of lignin fragments was chosen, driving the  
294 experiments by previous works done on lignin models (Brittain *et al.* 2018, Dabral *et al.*  
295 2018). However, to overcome the potential negative effects of impurities and lignin  
296 fragments distribution, we proceeded to the fractionation of Biolignin<sup>TM</sup> in order to  
297 obtain a purified fraction with a narrower distribution. This purified fraction is  
298 considered as a lignin model of the selected crude organosolv lignin.

299 **[Table 2]**

### 300 3.2. Purification of Biolignin<sup>TM</sup>

301 The aim of the fractionation was to isolate a homogeneous lignin fraction with a  
302 narrower molecular mass than Biolignin<sup>TM</sup> which can represent the pattern of  
303 Biolignin<sup>TM</sup> (*i.e.* same types of intra-linkages and reactive groups). Three fractions were  
304 isolated from the initial Biolignin<sup>TM</sup> by sequential extraction with diethyl ether (F1),  
305 dichloromethane (F2), methanol (Figure 2). The solid residue obtained after the last  
306 solvent extraction (*i.e.* Methanol) represented 29.0 ( $\pm 2.7$ )% w/w of the initial  
307 Biolignin<sup>TM</sup> sample and was highly insoluble in a large panel of organic solvents.

308 Methanol fraction represented the main part of the unfractionated material with a yield  
309 of 48.4 ( $\pm 2.2$ )% (w/w) while fractions F1 and F2 were respectively obtained with the  
310 yields of 6.4 ( $\pm 0.5$ )% and 16.2 ( $\pm 1.2$ )% w/w (Table 3). The four fractions were  
311 analyzed by Gel Permeation Chromatography (GPC) in order to determine their  
312 molecular weight. The results of GPC analysis (Table 3) showed that fractionation  
313 yielded fractions of increasing molecular weight. With a  $M_n$  and  $M_w$  of, respectively,  
314 611 and 784 g/mol, 747 and 1116 g/mol, 989 and 1579 g/mol, the distributions of the  
315 three first fractions were lower than the one of the initial Biolignin<sup>TM</sup> material ( $M_n$  999  
316 g/mol and  $M_w$  1743 g/mol). Fractions F1 and F2 gathered molecules with the lowest  
317 average molecular weight but did not yield a large part of the parent Biolignin<sup>TM</sup>  
318 ( $F1+F2 < 25\%$  (w/w)). Due to their low yield, these two fractions cannot be considered  
319 as a pattern of Biolignin<sup>TM</sup>.

320 According to the work of Lange and coworkers on wheat straw Biolignin<sup>TM</sup> (Lange et  
321 *al.* 2016), this lignin has an average molecular weight of a C9-unit of 162 g/mol. Even if  
322 the average number molecular weight ( $M_n$ ) of purified Biolignin<sup>TM</sup> and Biolignin<sup>TM</sup> are  
323 almost the same (*ca.* 6 C9-units), the average weight molecular weight ( $M_w$ ) decreases  
324 of one C9-unit in purified Biolignin<sup>TM</sup> (9.7 u *vs.* 10.8 u, respectively, Table 3). This  
325 offers us the opportunity to explore first the degradation conditions on the purified  
326 Biolignin<sup>TM</sup> that we consider as “lignin model” more homogeneous than its parent one.

### 327 [Table 3]

328 Thus, in regards to its GPC profile and its yield from Biolignin<sup>TM</sup>, the third fraction,  
329 named Purified Biolignin<sup>TM</sup> seemed to be a good candidate as a Biolignin<sup>TM</sup> model to  
330 optimize the degradation of lignin fragments by mechanochemistry. The chemical  
331 characterization of this fraction is described below.

332

333 *3.3. Composition and ATR-FT-IR of purified Biolignin<sup>TM</sup> fraction*

334 Biolignin<sup>TM</sup> and purified Biolignin<sup>TM</sup> are not entirely composed of lignin fragments.

335 However, after fractionation, purified Biolignin<sup>TM</sup> contains 31% less impurities than

336 Biolignin<sup>TM</sup> (8.94% vs. 12.92%, Table 4). This fractionation can thus be considered as

337 an efficient purification.

338 **[Table 4]**

339 In order to verify that purified Biolignin<sup>TM</sup> could be used to represent the behavior of

340 Biolignin<sup>TM</sup> during mechanochemical degradation, a comparison of the ATR-FT-IR

341 profile of purified and parent Biolignin<sup>TM</sup> was done. As it is indicated on Table 5, the

342 global shape of these two spectra were similar and perfectly fit with the usual IR profile

343 of lignins containing Guayacyl/Syringyl/ *p*-Hydroxyphenyl units (GSH-lignins) (Bykov

344 2008, Cronin et al. 2017). Then, the purification of Biolignin<sup>TM</sup> did not seem to drastically

345 modify the chemical structure of lignin fragments.

346 It could be noted that F1, F2 and the insoluble residue did not show an ATR-FT-IR profile

347 that totally fit with lignin profile. The only spectrum with some characteristic lignin IR

348 bands was the one of insoluble residue, however its global shape did not fit with the

349 Biolignin<sup>TM</sup> spectrum. See **Table S1** for more details.

350 **[Table 5]**

351

352 *3.4. NMR analysis of Biolignin<sup>TM</sup> and purified Biolignin<sup>TM</sup>*

353 Table 6 highlights the amount of hydroxyl groups and carboxylic acids quantified by

354 <sup>31</sup>P-NMR. The following signal ranges were integrated: 150.2-144.6, 143.7-140.2,

355 140.2-138.6, 138.6-136.9 and 135.6-133.7. They were attributed to, respectively,



356 aliphatic hydroxyls, phenolic hydroxyls of S-units and/or condensed G-units, G-units,  
357 H-units and carboxylic acids (Argyropoulos *et al.* 2021).

358 The  $^{31}\text{P}$ -NMR quantification supported the previous hypothesis that lignin fragments of  
359 Biolignin<sup>TM</sup> and Purified Biolignin<sup>TM</sup> are similar. However, a slight decrease of free  
360 phenolic hydroxyls of S-, condensed G- and G-units could be pointed on purified  
361 Biolignin<sup>TM</sup> compared to Biolignin<sup>TM</sup>. This loss of -0.25mmol/g will be considered in  
362 the following as too weak to influence the behavior of lignin fragments during their  
363 mechanochemical cleavage. Thus, the  $^{31}\text{P}$  NMR analysis validates the use of purified  
364 Biolignin<sup>TM</sup> as a model of Biolignin<sup>TM</sup> for the further the mechanochemical reactions.

365 **[Table 6]**

366 Several types of linkages exist in lignins. Their type and ratio are dependent on the plant  
367 source (Strassberger *et al.*, 2014). The most common linkages found in wheat straw  
368 Biolignin<sup>TM</sup> are shown in Figure 3.

369 With nearly 90% of the total identified linkages, the 3 major linkages in Biolignin<sup>TM</sup> and  
370 purified Biolignin<sup>TM</sup> are  $\beta$ -O-4' (**1**),  $\beta$ -5' (**2**) and  $\beta$ - $\beta$ ' (**3**) (Table 7). 1,2-Diarylpropane  
371 (**4**), monotetrahydrofuran (**5**) and  $\alpha,\beta$ -diarylether (**6**) represented only 7.4% and 10.9%  
372 of the total identified substructures in, respectively, Biolignin<sup>TM</sup> and Purified  
373 Biolignin<sup>TM</sup>.

374 With 69.7% and 73.6% of the identified substructures of, respectively, Biolignin<sup>TM</sup> and  
375 Purified Biolignin<sup>TM</sup> (Table 7),  $\beta$ -O-4' ether unit is the predominant linkage (Figure 3,  
376 Substructure **1**). This linkage is the most common one in lignin (40-70 wt%) and is  
377 among the most readily cleaved (Cui *et al.*, 2021). The energy necessary to cleave this  
378 linkage varies between 68.2 and 71.8 kcal/mol, depending on substitution pattern, which  
379 is weak compared to other lignin linkages (Sun *et al.*, 2018). The large presence and the

380 reactivity of  $\beta$ -O-4' lignin units have made them a target for many depolymerization/  
381 degradation strategies.

382 In view of this, we mainly focused on the cleavage of this linkage under mechano-  
383 chemical conditions. In this work, we did not optimize the experiments on the  
384 production of phenolic monomers, as it is largely described in the literature (Sun *et al.*,  
385 2018; Liu *et al.*, 2020). The aim of the study below is to decrease substantially the  
386 average molecular weight of Biolignin<sup>TM</sup> in order to enhance its ability to substitute  
387 phenol or polyols in various industrial applications. Halving the average molecular  
388 weight might be an acceptable goal to enhance the accessibility of functional groups for  
389 further coupling reactions.

390 The main goal of our study is to decrease the average molecular mass and the  
391 polydispersity of lignin fragments of an organosolv lignin source without highly  
392 modifying its functional groups content in order to avoid any decrease of its reactivity.  
393 This study is not trying to obtain platform molecules (vanillin etc..) from lignin but to  
394 partially depolymerize lignin fragments in order to optimize its use in applications  
395 (polyurethanes, phenolic resins, epoxy resins etc..) without any functional modification.

396 **[Table 7]**

397 **[Figure 3]**

398 *3.5. Mechanochemical cleavage of purified Biolignin<sup>TM</sup> with sodium hydroxide*

399 The double objective of this mechanochemical cleavage is to decrease the average  
400 relative molecular mass and the polydispersity of lignin fragments but also to optimize a  
401 protocol using cheap and widely available reagents. The literature highlighted  
402 promising results using sodium hydroxide to depolymerize an organosolv lignin (Kleine  
403 *et al.* 2013; Brittain *et al.* 2018). In contrast to Brittain and co-workers who tried to

404 optimize their experimental conditions in view of maximizing the production of  
405 monomers, this work focused on reaching a final homogeneous fraction, with roughly  
406 half of the original average molecular mass minimizing the condensation reaction as it  
407 could occur during lignin depolymerization (Li *et al.*, 2015). To our knowledge, only  
408 Fink *et al.* had the same approach using Kraft lignin with sodium percarbonate (Fink *et*  
409 *al.* 2023). In contrast to our study, Fink and co-workers worked on a Kraft lignin, which  
410 is highly branched, very heterogeneous and has higher average molar mass than  
411 organosolv lignins (~1500-25000 g/mol *vs.* 500-5000 g/mol for organosolv lignins) and  
412 consequently significantly less reactive than organosolv lignins. The author tried to  
413 cleave, to homogenize lignin fragments from Kraft lignin but also to increase some  
414 functional groups (mainly carbonyl groups) in order to improve its reactivity. In our  
415 case, Biolignin™ is already very reactive. The incorporation of new functional groups  
416 is unnecessary. The main point we focused on is the limitation of condensation reaction  
417 often observed during the depolymerization of lignin (Li *et al.*, 2015).  
418 In order to optimize the conditions of the reaction, purified Biolignin™ was chosen as  
419 an initial substrate. The experiments are described in Table 8.

#### 420 [Table 8]

##### 421 3.5.1 Optimization of the milling time and the quantity of sodium hydroxide

422 In their study, Brittain *et al.* (2014) used lignin and NaOH in an equimass ratio. In order  
423 to evaluate the performance of the degradation on purified Biolignin™, our four first  
424 experiments were also done with this ratio (Table 8, experiments D1 to D4) allowing a  
425 decrease of the average molecular mass of *ca.* 30% in only 15 min-milling and reach its  
426 lower average molecular mass after 60 min-milling (*ca.* -50%, See supporting  
427 information Fig. S1). However, the quantity of NaOH seem to be overdosed according

428 to the possible reaction mechanism between lignin and NaOH (Sun *et al.* 2020). Sodium  
429 hydroxide reacts with C<sub>β</sub>H of arylglycerol-β-arylether substructure (Figure 3,  
430 Substructure 1) by breaking β-O-4' linkage, the major linkage of purified Biolignin<sup>TM</sup>.  
431 It seems to be more consistent if a mole of NaOH is added for a mole of arylglycerol-β-  
432 arylether substructure (equimolar ratio). For convenience, we worked on the average  
433 C9-unit of Biolignin<sup>TM</sup> as the reference unit instead of the arylglycerol-β-arylether  
434 substructure. Lange *et al.* determined the average C9-unit of wheat straw Biolignin<sup>TM</sup> at  
435 162g/mol (Lange *et al.*, 2016). Thus, the experiments D5 to D10 (Table 8) were  
436 conducted with a molar ratio C9-unit/NaOH of 1:1 (D5, D7, D9) and 1:2 (D6, D8,  
437 D10). It is interesting to note that an equimass ratio purified Biolignin<sup>TM</sup>/ NaOH is  
438 equivalent to a 1:4 molar ratio C9-unit/NaOH. Decreasing NaOH quantity resulted in a  
439 final fraction with higher average molecular mass. Indeed, instead of a decrease of *ca.*  
440 50% after 60 min-milling, the average molar mass decreased of 28% and 36% for,  
441 respectively, 1:1 ratio C9-unit/NaOH (D7) and 1:2 ratio C9-unit/NaOH (D8). However,  
442 the study of FT-IR spectra gave some precious information (the normalized absorbances  
443 of measured FT-IR spectra can be found on Table S2). Sodium hydroxide cannot cause  
444 a ring cleavage, then, spectra were normalized against the vibration of the aromatic  
445 framework at 1510 cm<sup>-1</sup> which is supposed to not vary. A simultaneous decrease of  
446 intensity at 1210 cm<sup>-1</sup> (vibration of C-O-C) and 1140 cm<sup>-1</sup> (C-O stretch, Faix, O. 1991)  
447 indicates a cleavage of the ether bonds (Fink *et al.* 2023). Figure 4 represents the  
448 normalized FTIR absorption values of these two vibration bands exposed to different  
449 quantity of sodium hydroxide and time of milling. It clearly appeared that, after only 30  
450 min-milling, the equimass ratio purified Biolignin<sup>TM</sup>/ NaOH led to a significant increase  
451 of intensity at 1210 cm<sup>-1</sup> and 1140 cm<sup>-1</sup> while the (1:1) or (1:2) C9-unit/ NaOH molar

452 ratio show a decrease of these bands. Thus, it seemed that the milder conditions allowed  
453 the cleavage of ether bonds without any recombination of fragments while the use of an  
454 equimass quantity of NaOH leads to a cleavage of C-O-C bond quickly following by a  
455 rearrangement of new fragments, increasing the intensity at 1210 and 1140 cm<sup>-1</sup>.

456 **[Figure 4]**

457

458 Seeking to avoid any recombination of cleaved lignin fragments, the equimass ratio  
459 reaction was ruled out. According to GPC and FTIR analyses, the improvement of C-O-  
460 C cleavage between reactions with (1:2) and (1:1) C9-Units/NaOH was not sufficiently  
461 significant to favor the use of a (1:2) C9-Units/NaOH ratio.

462 Then, in the following, the mechanochemical reaction between lignin and sodium  
463 hydroxide will be equimolar (1:1 C9-Unit/NaOH), thus, leading to a drastic reduction of  
464 the quantity of NaOH (*i.e.* -75%) compared to the literature (Kleine *et al.* 2013, Brittain  
465 *et al.* 2018).

466

467 The three samples D5, D7 and D9, obtained after the (1:1) C9-unit/NaOH  
468 mechanochemical reaction were analyzed by HSQC NMR spectroscopy and compared  
469 with unmilled lignin sample. Figure 5 represents the evolution of the three main  
470 linkages ( $\beta$ -O-4',  $\beta$ -5' and  $\beta$ - $\beta'$ ) in which the aromatic unit (C9-unit) is defined as the  
471 internal standard (IS) of the sample. Indeed, aromatics are not supposed to vary during  
472 the discussed mechanochemical degradation because of their resistance to cleavage with  
473 NaOH. This method used a cluster of signals that are representative to all C9-units (*i.e.*  
474 IS) as following:

475  $I_{C9 \text{ units}} = 0.5IS_{2,6} + IG_2 + 0.5IH_{2,6}$ .

476 Where  $IS_{2,6}$  is the integration of  $S_{2,6}$ ,  $IG_2$  is the integral value of  $G_2$  and  $I_{H_{2,6}}$  is the  
477 integral value of  $H_{2,6}$ . This formula was determined by Wen and co-workers for grass  
478 lignin (Wen *et al.* 2012, Wen *et al.* 2013)

479  $I_{C9}$  represents the integral value of the aromatic ring. According to the internal standard  
480 ( $I_{C9}$ ), the amount of  $I_X\%$  could be obtained by the following formula:

$$481 \quad I_X\% = I_X/I_{C9} \times 100\%$$

482 Where  $I_X$  is the integral value of the  $\alpha$ -position of the substructures 1 ( $\beta$ -O-4), 2 ( $\beta$ -5),  
483 and 3 ( $\beta$ - $\beta$ ).

484 The inter-unit bonding spin system shows three different signals due to CH and  $CH_2$   
485 groups in the positions  $\alpha$ ,  $\beta$  and  $\gamma$  of the side chain (Figure 3).  $T_2$  relaxations of each  
486 signal is dependent on carbon substitution. Then, only the CH signals were selected for  
487 quantitative analyses. Among the CH signals for each spin system, we focused on the  
488 better-resolved resonances that did not overlap with signals. Hence, for quantification,  
489 the following signals were used: 1- $\alpha$ , 2- $\alpha$  and 3- $\beta$  (Figure 6). These selected signals are  
490 in accordance with those selected in literature (Sette *et al.* 2011).

491 **[Figure 5]**

492 **[Figure 6]**

493 Before milling, purified Biolignin<sup>TM</sup> contained, respectively, 20.5%, 4.3% and 1.6% of  
494 Arylglycerol- $\beta$ -arylether ( $\beta$ -O-4), Phenylcoumaran ( $\beta$ -5) and Resinol ( $\beta$ - $\beta$ ). After 2h of  
495 milling purified Biolignin<sup>TM</sup> without any presence of sodium hydroxide (C1  
496 experiment), this ratio reached 19.8%, 4.5% and 1.7% confirming that the mechanical  
497 energy given during the milling is insufficient to cleave lignin linkages.

498 Focusing on  $\beta$ -O-4' linkage, it clearly appeared that the main C-O-C cleavage occurred  
499 during the first 60 min of milling. Reaching 5.9% after 60 min of milling, more than

500 71% of the initial  $\beta$ -O-4' are cleaved. Then, with a slower degradation rate, more than  
501 86% of the initial  $\beta$ -O-4' are cleaved after 120 min of milling. Considering the energy  
502 cost of milling (Sealy *et al.* 2016) and setting the milling duration at 60 min seemed  
503 more beneficial from the perspective of the process scale-up to industrial scale.  
504 We expected that resinol (Substructure 3,  $\beta$ - $\beta'$  linkage) was not impacted by the  
505 degradation, because of the resistance of C-C bonds to cleavage with basic catalysts  
506 (Zakzeski *et al.* 2010, Kleine *et al.* 2013). However, the HSQC quantification seemed to  
507 indicate that a cleavage of this linkage occurred. From 2.0% before milling, this linkage  
508 reached 0.2% after 60 min of milling. After 120 min of milling, an odd phenomenon  
509 appeared: the quantity of  $\beta$ - $\beta'$  linkage increased until reaching 0.8%. It may indicate  
510 that some slight rearrangements occurred after 60 min of milling.  
511 Phenylcoumaran (Substructure 2,  $\beta$ -5' linkage) was also affected by the  
512 mechanochemical degradation. From 4.3% before milling, this linkage slowly  
513 decreased, reaching 1.9%, then 1.4% after, respectively 60 min and 120 min of milling.  
514 The above discussed cleavages were visually observed on Figure 6 where the intensity  
515 of correlation spots of 1- $\alpha$ , 2- $\alpha$  and 3- $\beta$  progressively decreased with the milling time.  
516 Hence, in view of the above results, the best compromise between the efficiency of the  
517 cleavage of purified Biolignin<sup>TM</sup> and the quantity of sodium hydroxide/ time of milling  
518 was the use of an equimolar ratio C9-unit/NaOH during 60 min of milling.

519

### 520 3.5.2 Influence of moisture content

521 Cleavage of lignin is mainly a hydrolysis reaction under strong basic conditions  
522 (Klapiszewski *et al.* 2018). A molecule of water is required for each C-O-C bond  
523 cleavage. In the present study, the moisture content of Purified Biolignin<sup>TM</sup> was

524 increased from 4 wt% (D7, initial moisture of Purified Biolignin<sup>TM</sup>) to 24% (D14)  
525 (Table 8) by adding water with purified Biolignin<sup>TM</sup> and sodium hydroxide in the two  
526 jars before grinding. Mechanochemistry has the advantage of being a solvent-free  
527 technique. However, adding a small amount of liquid could enhance the reactivity. In  
528 order to be considered as a solvent-free reaction, it has to respect the Liquid-Assisted  
529 Grinding (LAG) zone (*i.e.*  $0 < \eta < 2 \mu\text{L}/\text{mg}$ ) (Ying *et al.* 2021). Beyond  $\eta = 2 \mu\text{L}/\text{mg}$ , the  
530 added solvent is too high to consider the reaction as solvent-free. The solvent could  
531 slurring the medium and affect the efficiency of the grinding. The  $\eta$  value was  
532 calculated for each experiment in order to always respect the LAG condition. The  
533 calculated  $\eta$  value is indicated on Table 8.

534 The average relative molecular mass of the grinded samples with an increase of  
535 moisture (D7 to D14) is illustrated on Table 9.

536 Surprisingly, the average molecular mass of milled sample constantly decreases until  
537 D13, the experiment with a moisture content of 18 wt%. At this point, the  
538 mechanochemical reaction allowed an average molecular mass reduction of *ca.* 40%, in  
539 other words it allowed the obtention of a fraction with lignin fragments with *ca.* 4 C9-  
540 units. Keeping on mind the industrialization of the process, this is a particularly  
541 interesting result because it could suggest the use of a less dry lignin, thus implying  
542 much less energy cost compared to the actual one for lignin drying,

543 When the sample contains 24 wt% of water (Experiment D14), the average molecular  
544 mass increases, reaching the same weight, or even worse, than D7, the sample with only  
545 4 wt% water. However, this phenomenon was already observed by Brittain and co-  
546 workers (Brittain *et al.* 2018). For higher percentage of water (*i.e.*  $\geq 24 \text{ wt}\%$  in the



547 present study), the mixture grinded is no longer a powder but rather a slurry affecting  
548 the efficiency of the mechanochemical conditions as it was on lignin/NaOH powder.

549 **[Table 9]**

### 550 *3.5.3 Influence of methanol as a scavenger for reactive intermediates*

551 In the literature, the biggest challenge of lignin depolymerization is to avoid  
552 repolymerization/ condensation reactions. Lignin hydrolysis with a basic catalyst  
553 generates unstable intermediates. These reactive intermediates are easily recombined in  
554 new oligomers with C-C linkages, unbreakable in the presence of basic catalysts (Li et  
555 *al.* 2015).

556 Brittain and co-workers (Brittain et *al.* 2018) had promising results using methanol as a  
557 scavenger to prevent any repolymerization reaction during the milling of lignin and  
558 sodium hydroxide. In their study, they added 0.40 mL of methanol for 1.50 g of lignin  
559 and 1.50 g of sodium hydroxide, so 0.27 $\mu$ L/mg of lignin. They observed a quicker and a  
560 more efficient depolymerization, with a final average relative molecular mass 40%  
561 smaller compared to the samples milled with sodium hydroxide in absence of methanol.  
562 In the following, methanol was added before the reaction between Purified Biolignin<sup>TM</sup>  
563 and sodium hydroxide using (1:1) C9-Unit/NaOH ratio ( $\eta = 0.27\mu\text{L/mg}$  of lignin). Two  
564 milling time were tested, 30 min (D15) and 60 min (D16), and compared with the  
565 samples milled without methanol (*i.e.* D5, D7 and D13, Table 8). The average  
566 molecular mass of the compared samples is shown in Table 10).

567 **[Table 10]**

568 Two samples, D5 and D15, were milled during 30 minutes without and in the presence  
569 of methanol. The results obtained indicated that methanol increases obviously the rate  
570 of depolymerization. With only 30 min of milling, the presence of methanol to the

571 system allowed the recovery of lignin fragments 29% smaller than in its the absence (in  
572 regards to  $M_n$  value). However, contrary to Brittain *et al.* (2018) findings, milling for a  
573 longer time in presence of methanol (*i.e.* D16, 60 min of milling) did not improve the  
574 efficiency of the depolymerization. The obtained fragments had nearly the same average  
575 relative molecular mass than those obtained after 30 min of milling. A slight increase of  
576 FTIR bands  $1210\text{ cm}^{-1}$  and  $1140\text{ cm}^{-1}$  between D15 and D16 indicated that D16 contains  
577 more C-O-C linkages than D15 (See Supporting information, Table S2). According to  
578 Aboagye and co-workers, this could be the result of additional methoxy groups  
579 (Aboagye *et al.* 2023). Concerning our experiment, the band on D16 FTIR spectrum is  
580 7% and 12% higher than D15 FTIR and Purified Biolignin<sup>TM</sup> spectrum.

581

582 It is interesting to note that D13 experiment (60 min milling with 18 wt% H<sub>2</sub>O, without  
583 MeOH) gave same, or slightly smaller lignin fragments than those obtained by D15  
584 experiment (30 minutes milling with a dry lignin and the presence of MeOH). In view  
585 of these results and considering an environmentally friendly process, it seems more  
586 advantageous to optimize the process without the presence of methanol, even if the  
587 needed milling time is twice longer.

588

### 589 3.6. Mechanochemical cleavage of Biolignin<sup>TM</sup> with sodium hydroxide

#### 590 3.6.1. Reaction on P7 Premium Line ball mill (20 mL ZrO<sub>2</sub> jars with 5 ZrO<sub>2</sub> balls)

591 The promising results obtained using purified Biolignin<sup>TM</sup> encouraged us to directly test  
592 the mechanochemical cleavage on Biolignin<sup>TM</sup>, without any prior purification (C2, D17,  
593 D18, 19, Table 11). The experiments were tested on Biolignin<sup>TM</sup> using the same  
594 planetary mill as above (Fritsch Pulverisette 7 Premium Line ball mill). For C2

595 experiment, Biolignin<sup>TM</sup> was milled without sodium hydroxide. The average relative  
596 molecular mass of the recovered sample confirms that grinding Biolignin<sup>TM</sup> without the  
597 presence of an appropriate reagent did not allow a significant depolymerization.  
598 Concerning the experiment D19, using a Biolignin<sup>TM</sup> of 18 wt% of H<sub>2</sub>O, the reaction  
599 mixture was not recoverable. After milling, a very sticky slurry surrounded the balls.  
600 The scale up of such process seemed to be too hazardous to be considered. Most  
601 gratifyingly, the mechanochemical cleavage of Biolignin<sup>TM</sup>, without its prior  
602 purification, afforded lignin fragments in final samples *ca.* 40% smaller than in the  
603 initial Biolignin<sup>TM</sup> (Table 11), indicating the presence of oligomers with less than 4 C9-  
604 units in average.  
605 Comparison of 4%wt and 14%wt water (D17, D18 experiments respectively) showed  
606 that  $M_n$  values are similar while  $M_w$  showed 10% decrease for experiment D18 with  
607 14%wt water (Table 11). Using a wetter lignin did not significantly affect the  $M_n$  value  
608 of the milled sample but decrease the  $M_w$ , resulting the recovery of a more  
609 homogeneous fraction.  
610 Most importantly, our findings indicate the same decrease as the optimized reaction  
611 with purified Biolignin<sup>TM</sup> (D13, Purified Biolignin<sup>TM</sup>/ NaOH 1:1 C9-unit/NaOH + 18  
612 wt% H<sub>2</sub>O, 60 min milling, Table 9) was observed.

613 **[Table 11]**

614 Before milling, Biolignin<sup>TM</sup> contained, respectively, 16.8/100 C9, 4.9/100 C9 and  
615 1.3/100 C9 of Arylglycerol- $\beta$ -arylether ( $\beta$ -O-4'), Phenylcoumaran ( $\beta$ -5') and Resinol  
616 ( $\beta$ - $\beta'$ ). After 60 min of milling and in the presence of 4% (w/w) and 14% (w/w) of H<sub>2</sub>O,  
617 the occurrence of  $\beta$ -O-4' decreased of 38% and more than 44%, respectively (Figure 7).  
618 These decreases were weaker than those observed on Purified Biolignin<sup>TM</sup>, however,

619 Biolignin<sup>TM</sup> contains more hemicelluloses than purified Biolignin<sup>TM</sup>. A part of NaOH  
620 was probably used to cleave C-O-C linkages between lignin fragments and  
621 hemicellulose. The <sup>31</sup>P-NMR spectrum gave also some precious information.  
622 The 4-O-5' linkage of condensed G-units significantly decreased (Table 12) while the  
623 other moieties seemed almost constant before and after the mechanochemical  
624 degradation. Surprisingly, the <sup>31</sup>P-NMR spectrum seemed to indicate NaOH cleavage of  
625 C-O-C of 4-O-5' linkage. This cleavage was not distinguished by HSQC analysis  
626 because no HSQC correlations are observed for carbons in positions 4, 4', 5 and 5' of  
627 the aromatics. The combination of both NMR techniques was thus essential for a better  
628 understanding of all the different cleavages produced during the reaction.  
629 The <sup>31</sup>P-NMR spectrum also confirmed that reactive groups of Biolignin<sup>TM</sup> (mostly  
630 phenolic and aliphatic OH) are almost unchanged after degradation (Table 12). This  
631 point was primordial to validate the degradation without affecting the reactivity of the  
632 sample.  
633 The C-O-C cleavage of β-O-4' linkage seemed to be improved when Biolignin<sup>TM</sup>  
634 moisture is increased ((i.e. 14% H<sub>2</sub>O (w/w) vs. 4% H<sub>2</sub>O (w/w)). This is an interesting  
635 result that encourages us to reduce the Biolignin<sup>TM</sup> drying rate.

636 **[Figure 7]**

637 In view of the above results, using a mechanical reaction with sodium hydroxide,  
638 impurities of Biolignin<sup>TM</sup> do not impact on the efficient cleavage of lignin fragments.

639 **[Table 12]**

640 *3.6.2. Scale up and Optimization of the reaction between Biolignin<sup>TM</sup> and NaOH on*  
641 *Retsch PM 100 ball mill*

642

643 The positive results described above were enough encouraging to scale up the reaction  
644 to the planetary 500 mL mill available in the CIMV lab (Retsch PM 100 ball mill  
645 equipped with a tungsten carbide (WC) jar and 20 mm diameter WC balls). The  
646 maximum RPM of this mill is 650, 150 RPM less than the previous planetary mill used.  
647 The density of WC (14.80 g/cm<sup>3</sup>) is higher than ZrO<sub>2</sub> (6.05 g/cm<sup>3</sup>), thus providing in  
648 principle better results due to the capability of imparting strong impact forces to the  
649 particles (Sitotaw et al. 2023). Then, the large scale mechanochemical cleavage of  
650 Biolignin<sup>TM</sup> was tested adapting some parameters to the available materials. Instead of  
651 650 mg, the initial Biolignin<sup>TM</sup> added to the system was 17.000g, a 26-fold greater  
652 quantity than in prior experiments (Table 13).

653 **[Table 13]**

654 At the beginning, 10 WC balls was used at 650 RPM during 60 minutes (D20). The  
655 milled sample recovered after this experiment has lignin fragments 41-45% smaller than  
656 those of the initial Biolignin<sup>TM</sup> (Table 13). This was the smallest lignin fragments  
657 recovered from all our experiments described above.

658 In order to improve the reaction, 20 WC balls (Experiment D21) were used instead of  
659 the initial 10 WC balls (Experiment D20). Increasing the number of ball mills gave  
660 positive results. The recovery fraction contained an average of trimers of lignin (51-  
661 55% smaller than the initial Biolignin<sup>TM</sup>). A lignin fraction containing trimers seems to  
662 be very promising to improve its use on applications avoiding issues of sterically  
663 shielded reactive groups.

664 **[Figure 8]**

665 After 60 min of milling with 10 WC-balls and 20 WC-balls in the WC-500mL jar, the  
666 occurrence of  $\beta$ -O-4' linkages decreased of 35.4% and more than 51.0%, respectively

667 (Figure 8). Hence, doubling the number of milling balls allowed a significant decrease  
668 of occurrence of  $\beta$ -O-4' linkages.

669 So, to summarize this part, the final protocol allowed to halve the average molecular  
670 mass of lignin fragments and to halve the occurrence of  $\beta$ -O-4' linkages of Biolignin™  
671 without any prior purification.

672

#### 673 **4. Conclusion**

674 Our study aimed to decrease by mechanochemical means the average molecular mass  
675 and the polydispersity of lignin fragments of the organosolv lignin named Biolignin™,  
676 without highly impacting its functional groups content. This is the first mechano-  
677 chemical study on this kind of lignin. The reaction was firstly optimized on “purified  
678 Biolignin™”, containing more uniform lignin fragments and less impurities than  
679 Biolignin™. Comparative studies between Biolignin™ and purified Biolignin™ by  
680 their ATR-FT-IR profile and by <sup>31</sup>P-NMR quantification demonstrated that the chemical  
681 structure of their lignin fragments is similar, thus validating the use of purified  
682 Biolignin™ as a model of Biolignin™.

683 For both studies on purified Biolignin™ and Biolignin™, quantitative HSQC NMR, IR  
684 and GPC studies, supported our findings.

685 An important point highlighted by our study is the efficiency of the reaction when using  
686 an equimolar quantity (and not equimass) of sodium hydroxide related to C-9 unit of  
687 Biolignin™ needed to break interunits lignin bonds. This corresponds to a 75%  
688 reduction of sodium hydroxide quantity compared to the literature. Under these  
689 conditions and after 60 min-grinding in the planetary ball milling apparatus, more than  
690 71% of the initial  $\beta$ -O-4' bonds are cleaved.

691 The effect of Liquid Assisted Grinding (LAG), using water or methanol, showed a  
692 slightly better result with water. The mechanochemical reaction with a 18 wt% moisture  
693 content allowed an average molecular mass reduction of *ca.* 40%, indicating the  
694 obtention of lignin fragments with *ca.* 4 C<sub>9</sub>-units. Analogous results were observed on  
695 Purified Biolignin<sup>TM</sup> and on Biolignin<sup>TM</sup>.

696 Mechanochemical results with Biolignin<sup>TM</sup> under LAG conditions are particularly  
697 important. Obtention of Biolignin<sup>TM</sup> at 18 wt% moisture content implies much less  
698 energy input needed. This, in conjunction with the use of an equimolar ratio of sodium  
699 hydroxide could be the base of an economically feasible industrialized process for the  
700 mechanochemical cleavage Biolignin<sup>TM</sup>.

701 Finally, for the first time the mechanochemical cleavage was conducted in a planetary  
702 500mL mill. For a total of 14 wt% moisture on Biolignin<sup>TM</sup> and an equimolar amount of  
703 sodium hydroxide, a 60 min grinding afforded halve (-51%) the average molecular mass  
704 of lignin fragments and decreased for more than 44% the occurrence of β-O-4' linkages  
705 in lignin fragment, suggesting the feasibility of scaling-up.

706 The significant improvements (sodium hydroxide reduction and moisture precise  
707 content) can pave the way for using less energetically demanding process for obtaining  
708 Biolignin<sup>TM</sup> and also envision an industrial scale up for lignin cleavage.

709 In addition, we envision to explore in the near future the combined opportunities that  
710 might be offered by our results and the potential oxidative cleavage of Biolignin<sup>TM</sup>.

## 711 **Acknowledgements**

712 The authors are grateful to the Centre National de la Recherche Scientifique (CNRS)  
713 and the Université Paul Sabatier for financial support. The authors (N.C., M.B., B.B.-

714 M.) are particularly thankful to French Government, the CNRS and the ANR (Agence  
715 Nationale de Recherche) for financing this work through the “Plan Préservation  
716 Emplois R&D - 2236394\_CIMV\_upr8241 LCC - DRARI-31-300; project: “Catalyzed  
717 degradation of lignin”. The authors thank the members of the CIMV technical team for  
718 their contribution to the experimental data and Dr. Dominique Agustin (Associate  
719 Professor, LCC, Laboratoire de Chimie de Coordination, Team G “Ligands, complex  
720 architectures and catalysis” for fruitful discussions on this part of the project.

721

## 722 **Appendix A. Supplementary data**

723 Supplementary data associated with this article can be found in the online version.

724

## 725 **References**

726 Abdelaziz, O.Y., Clemmensen, I., Meier, S., Costa, C.A.E., Rodrigues, A., Hultberg,  
727 C.P., Riisager, A., 2022. On the Oxidative Valorization of Lignin to High-Value  
728 Chemicals: A Critical Review of Opportunities and Challenges. *Chem. Sust. Chem.* 15,  
729 1-20. DOI: 10.1002/cssc.202201232

730

731 Aboagye, D., Medina, F., Contreras, S., 2023. Toward a facile depolymerization of  
732 alkaline lignin into high-value platform chemicals via the synergetic combination of  
733 mechanocatalysis with photocatalysis or Fenton process. *Catal. Today*, 413-415. DOI:  
734 10.1016/j.cattod.2022.11.030

735

736 Argyropoulos, D.S., Pajer, N., Crestini, C., 2021. Quantitative <sup>31</sup>P NMR Analysis of  
737 Lignins and Tannins. *JoVE* 174, 1-21, DOI: 10.3791/62696

738

739 Benjelloun-Mlayah, B., Delmas, M., 2019. Method of production of lignin and  
740 hemicellulose from a plant lignocellulosic material. Patent No WO2019162277A1

741



742 Brittain, A.D., Chrisandina, N.J., Cooper, R.E., Buchanan, M., Cort, J.R., Olarte, M.V.,  
743 Sievers, C., 2018. Quenching of reactive intermediates during mechanochemical  
744 depolymerization of lignin. *Catal. Today* 302, 180-189. DOI:  
745 10.1016/j.cattod.2017.04.066  
746  
747 Bykov, Y. 2008. Characterization of natural and technical lignins using FTIR  
748 spectroscopy. Master's Thesis Dissertation. Retrieved from  
749 <https://urn.kb.se/resolve?urn=urn:nbn:se:ltu:diva-42881>  
750  
751 Cachet, N., Benjelloun-Mlayah, B., 2021. Comparison of organic acid-based organosolv  
752 lignins extracted from the residues of five annual crops. *Bioresources* 16 (4), 7966-7990.  
753 DOI: 10.15376/biores.16.4.7966-7990  
754  
755 Cronin, D. J., Dunn, K., Zhang, X., Doherty, W. O. S., 2017. Relating Dicarboxylic Acid  
756 Yield to Residual Lignin Structural Features. *ACS Sustain. Chem. Eng.* 5 (12), 11695–  
757 11705. DOI: 10.1021/acssuschemeng.7b03164  
758  
759 Cui, Y., Goes, S.L., and Stahl, S.S., 2021. Sequential Oxidation-Depolymerization  
760 Strategies for Lignin Conversion to Low Molecular Weight Aromatic Chemicals. *Adv.*  
761 *Inorg. Chem.* 77, 99-136 DOI: 10.1016/bs.adioch.2021.02.003  
762  
763 Dabral, S., Wotruba, H., Hernandez, J.G., Bolm, C., 2018. Mechanochemical oxidation  
764 and cleavage of lignin  $\beta$ -O-4 model compounds and Lignin. *ACS Sustain. Chem. Eng.* 6,  
765 3242-3254. DOI: 10.1021/acssuschemeng.7b03418  
766  
767 Faix, O., 1991. Classification of lignins from different botanic origins by FT-IR  
768 spectroscopy. *Holzforschung* 45 Suppl., 21-27.  
769  
770 Fink, F., Stawski, T.M., Stockmann, J.M., Emmerling, F., Falkenhagen, J., 2023. Surface  
771 modification of Kraft lignin by mechanochemical processing with sodium percarbonate.  
772 *BioMacromolecules* 24, 4274-4284. DOI: 10.1021/acs.biomac.3c000584  
773

774 Klapiszewski, L., Szalaty, T.J., Jesionowski, T., 2018. Chap. 1 Depolymerization and  
775 Activation of Lignin: Current State of Knowledge and Perspectives. In “Lignin Trends  
776 and Applications” DOI: 10.5772/intechopen.70376  
777

778 Kleine, T., Buendia, J., Bolm, C., 2013. Mechanochemical degradation of lignin and  
779 wood by solvent-free grinding in a reactive medium. *Green Chem.* 15, 160-166. DOI:  
780 10.1039/c2gc36456e  
781

782 Lange, H., Schiffels, P., Sette, M., Sevastyanova, O. and Crestini, C., 2016. Fractional  
783 Precipitation of Wheat Straw Organosolv Lignin: Macroscopic Properties and Structural  
784 Insight. *ACS Sustain. Chem. Eng.* 4(10), 5136-5151  
785

786 Llovera, L., Benjelloun-Mlayah, B., Delmas, M., 2016. Organic acid lignin-based  
787 polyurethane films: Synthesis parameter optimization. *Bioresources* 11(3), 6320-6334.  
788

789 Li, C., Zhao, X., Wang, A., Huber, G.W., Zhang, T., 2015. Catalytic Transformation of  
790 Lignin for the Production of Chemicals and Fuels. *Chem. Rev.* 115 (21), 11559–11624.  
791 DOI: 10.1021/acs.chemrev.5b00155  
792

793 Liu, X., Bouxin, F.P., Fan, J., Budarin, V.L., Hu, C. and Clark, J.H., 2020. Recent  
794 Advances in the Catalytic Depolymerization of Lignin towards Phenolic Chemicals: A  
795 Review. *Chem. Sus. Chem.* 13, 4296-4317. DOI: 10.1002/cssc.202001213  
796

797 Marriotti, F., Tomé, D., and Mirand, P., 2008. Converting Nitrogen into Proteins -  
798 Beyond 6.25 and Jones' factors. *Crit. Rev. Food Sci. Nutr.* 48, 177-184. DOI:  
799 10.1080/10408390701279749  
800

801 Sealy, M.P., Liu, Z.Y., Zhang, D. Guo, Y.B., Liu, Z.Q., 2016. Energy consumption and  
802 modeling in precision hard milling. *J. Clean. Prod.* 135, 1591-1601. DOI:  
803 10.1016/j.jclepro.2015.10.094  
804

805 Sette, M., Wechselberger, R., and Crestini, C., 2011. Elucidation of lignin structure by  
806 quantitative 2D NMR. *Chem. Eur. J.* 17, 9529-9535. DOI: 10.1002/chem.201003045  
807

808 Sitotaw, Y.W., Habtu, N.G., Gebreyohannes, A.Y., Nunes, S., Gerven, T.V., 2023. Ball  
809 milling as an important pretreatment technique in lignocellulose biorefineries: a review.  
810 *Biomass Convers. Biorefin.* 13, 15593-15616. DOI: 10.1007/s13399-021-01800-7  
811

812 Sluiter, A., Hames, B. R, Scarlata, C., Sluiter, J., Templeton, D., and Crocker, D., 2008.  
813 Determination of structural carbohydrates and lignin in biomass, in: *Laboratory*  
814 *Analytical Procedure (LAP)*. National Renewable Energy Laboratory.  
815

816 Strassberger, Z., Tanase, S. and Rothenberg, G., 2014. The Pros and Cons of Lignin  
817 Valorization in an Integrated Biorefinery. *RSC Adv.* 4, 25310–25318.  
818

819 Sun, C., Zheng, L., Xu, W., Dushkinb, A.V., and Su, W., 2020. Mechanochemical  
820 cleavage of lignin models and lignin via oxidation and a subsequent base-catalyzed  
821 strategy. *Green Chem.* 22, 3489–3494. DOI: 10.1039/d0gc00372g  
822

823 Sun, Z., Fridrich, B., de Santi, A., Elangovan, S. and Barta, K., 2018. Bright Side of  
824 Lignin Depolymerization: Toward New Platform Chemicals. *Chem. Rev.* 118, 614-678.  
825 DOI: 10.1021/acs.chemrev.7b00588  
826

827 Tachon, N., Benjelloun-Mlayah, B., Delmas, M., 2016. Organosolv wheat straw lignin as  
828 a phenol substitute for green phenolic resins. *Bioresources* 11(3), 5797-5815 DOI:  
829 10.15376/biores.11.3.5797-5815  
830

831 Wen, J.-L., Xue, B.-L., Xu, F., Sun, R.-C., 2012. Unveiling the structural heterogeneity  
832 of bamboo lignin by in situ HSQC NMR technique. *Bioenergy Res.* 5, 886–903. DOI:  
833 10.1007/s12155-012-9203-5  
834

835 Wen, J.-L., Sun, S.-L., Xue, B.-L., and Sun, R.-C., 2013. Recent Advances in  
836 characterization of lignin polymer by solution-state Nuclear Magnetic Resonance (NMR)  
837 methodology. *Materials* 6, 359-391. DOI: 10.3390/ma6010359  
838

839 Xu, W., Zhou, C., Hu, K., Yang, J. Su, W., Qiao, P., 2023. Novel Mechanoenzymatic  
840 Strategy for Lignin Depolymerization. *Ind. Eng. Chem. Res.* 62(46), 19448-19458. DOI:  
841 10.1021/acs.iecr.3c02959  
842

843 Ying, P., Yu, J., Su, W., 2021. Liquid-Assisted Grinding Mechanochemistry in the  
844 Synthesis of Pharmaceuticals. *Adv. Synth. Catal.* 363, 1246-1271. DOI:  
845 10.1002/adsc.202001245  
846

847 Zakzeski, J., Bruijninx, P.C.A., Jongerius, A.L., Weckhuysen, B.M., 2010. The  
848 Catalytic Valorization of Lignin for the Production of Renewable Chemicals. *Chem.*  
849 *Rev.* 110, 6, 3552-3599. DOI: 10.1021/cr900354u  
850

851 Zhou, N., Thilakarathna, W.P.D.W., He, Q.S., Rupasinghe, H.P.V., 2022. A Review:  
852 Depolymerization of lignin to generate High-value bio-products: Opportunities,  
853 Challenges, and Prospects. *Front. Energy Res.* 9, Article 758744. DOI:  
854 10.3389/fenrg.2021.758744

1 **Mechanochemical cleavage of lignin in presence of sodium hydroxide**  
2 **to produce a homogeneous lignin fraction optimized for a direct use in**  
3 **applications**

4 Nadja Cachet<sup>1,3</sup>, Pierre Lavedan<sup>2</sup>, Michel Baltas<sup>3\*</sup>, Bouchra Benjelloun-Mlayah<sup>1\*</sup>

5

6 <sup>1</sup> CIMV, 109 rue Jean Bart, Diapason A, F-31670 Labège, France

7 <sup>2</sup> Institut de Chimie de Toulouse, UAR 2599, 118 Route de Narbonne, Toulouse Cedex  
8 09, 31062, France

9 <sup>3</sup> CNRS, LCC (Laboratoire de Chimie de Coordination), Université de Toulouse, UPS,  
10 205 Route de Narbonne, BP 44099, Cedex 4, 31077 Toulouse, France

11 \* Corresponding authors Email: michel.baltas@lcc-toulouse.fr; b.benjelloun@cimv.fr

12

13 **Figure captions**

14 **Fig. 1.** CIMV organosolv biorefinery process

15 **Fig. 2.** Scheme of fractionation of the Biolignin<sup>TM</sup>

16 **Fig. 3.** 6 main lignin moieties present in Biolignin<sup>TM</sup> and Purified Biolignin<sup>TM</sup>

17 **Fig. 4.** Normalized FTIR absorption values of Alkyl-aryl ether asymmetric C-O  
18 vibration (1210 nm) and C-O stretching (1140 nm) exposed to different quantity of  
19 sodium hydroxide

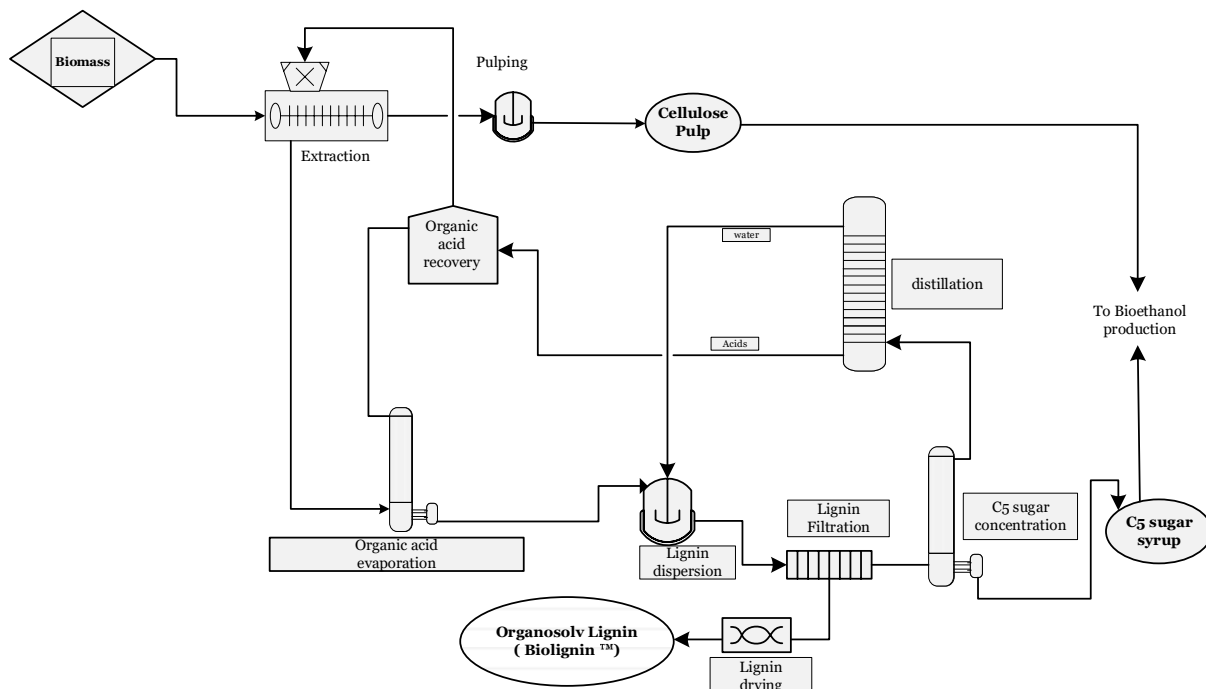
20 **Fig. 5.** Evolution of the 3 main linkages of lignin samples ( $\beta$ -O-4',  $\beta$ -5' and  $\beta$ - $\beta$ ')  
21 determined by quantitative HSQC (/100 C9 unit)

22 **Fig. 6.** HSQC NMR Spectra of Purified Biolignin<sup>TM</sup> before milling (a); after 120 min  
23 milling without the presence of NaOH (C1, b), and with NaOH after 30 min milling  
24 (D5, c), 60 min milling (D7, d), 120 min milling (D9, e)

25 **Fig. 7.** Occurrence of  $\beta$ -O-4',  $\beta$ -5' and  $\beta$ - $\beta$ ' (/100 C9 unit) in Biolignin<sup>TM</sup>, D17 and D18  
26 as determined by quantitative NMR HSQC

27 **Fig. 8.** Occurrence of  $\beta$ -O-4',  $\beta$ -5' and  $\beta$ - $\beta'$  (/100 C9 unit) in Biolignin<sup>TM</sup>, after milling  
 28 with 10 balls and 20 balls as determined by quantitative NMR HSQC

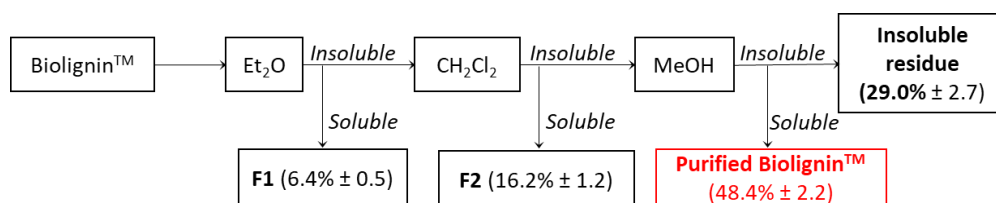
29



30

31 **Figure 1** – CIMV organosolv biorefinery process

32

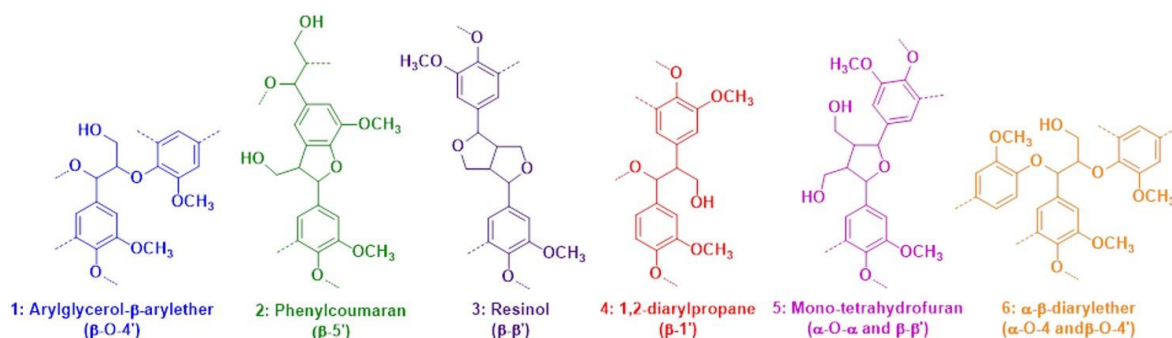


33

34

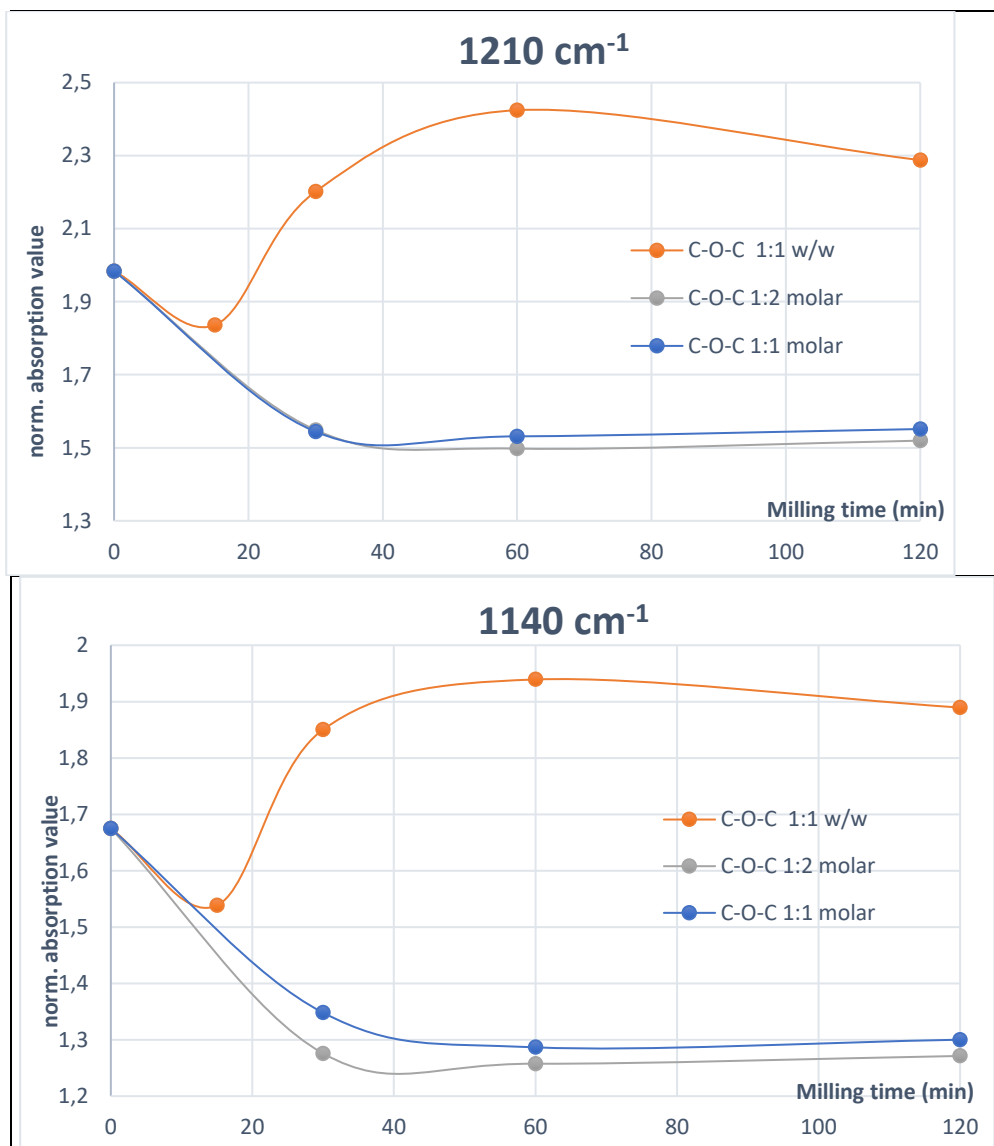
35 **Figure 2** – Scheme of fractionation of the Biolignin<sup>TM</sup>

35



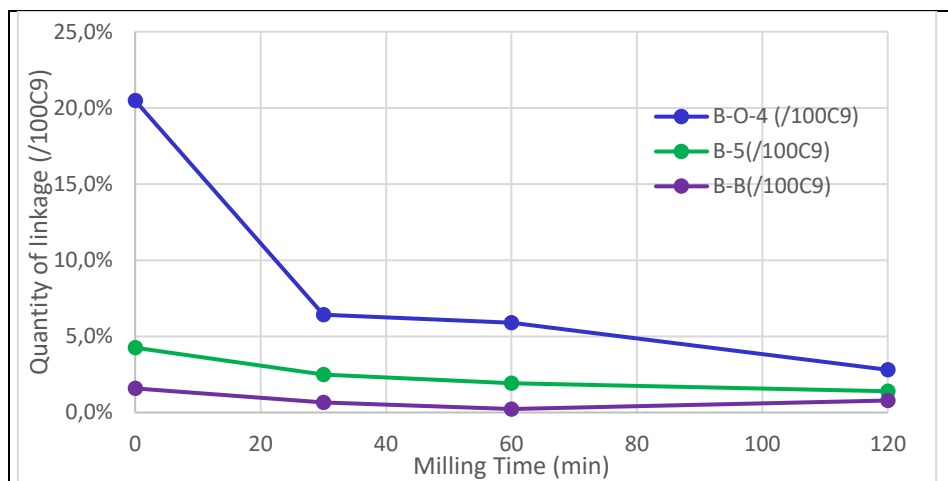
36

37 **Figure 3** – 6 Main lignin moieties present in Biolignin<sup>TM</sup> and Purified Biolignin<sup>TM</sup>



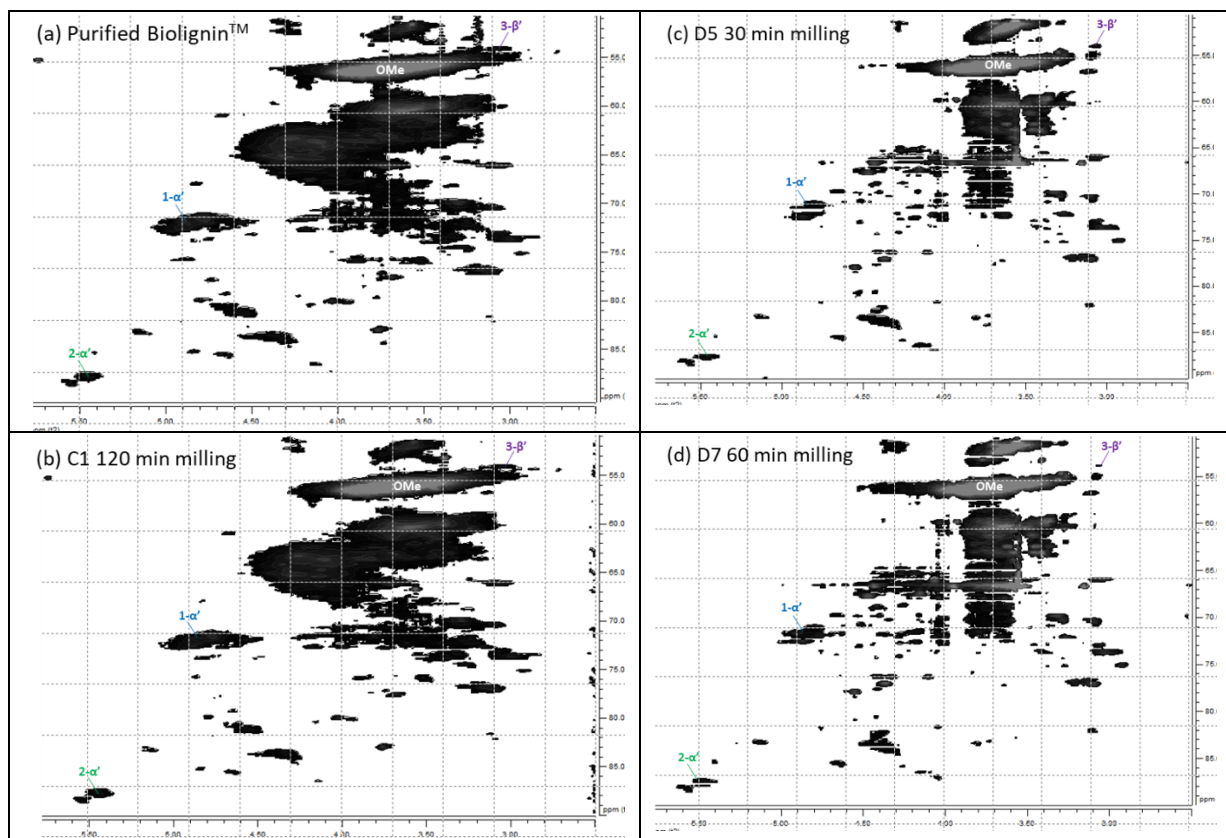
38 **Figure 4** – Normalized FTIR absorption values of Alkyl-aryl ether asymmetric C-O  
 39 vibration (1210 nm) and C-O stretching (1140 nm) exposed to different quantity of  
 40 sodium hydroxide  
 41  
 42

	Milling Time (min)	I <sub>β-04'</sub> (/100C9)	I <sub>β-5'</sub> (/100C9)	I <sub>β-β'</sub> (/100C9)
Purified Biolignin™	0	20.5	4.3	1.6
D5	30	6.4	2.5	0.7
D7	60	5.9	1.9	0.2
D9	120	2.8	1.4	0.8

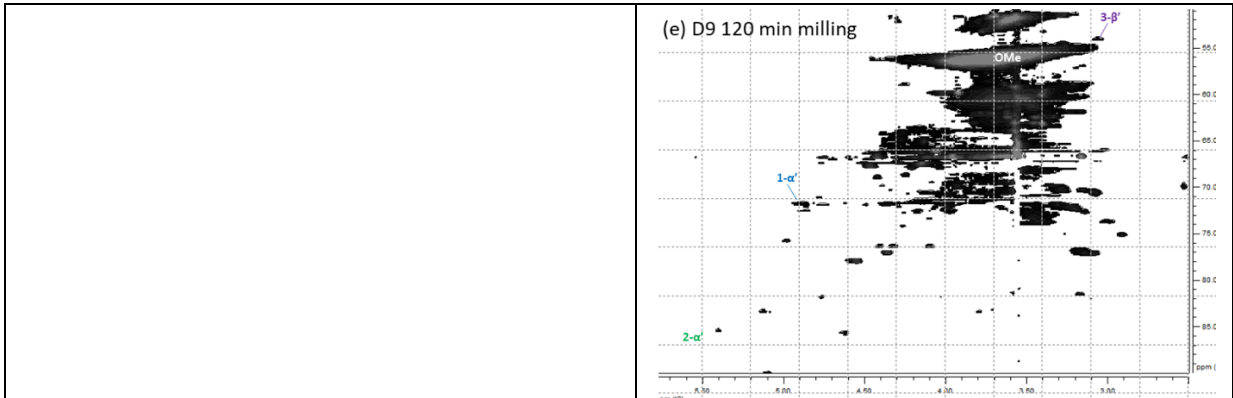


43 **Figure 5** – Evolution of the 3 main linkages of lignin samples ( $\beta$ -O-4',  $\beta$ -5' and  $\beta$ - $\beta$ ')  
 44 determined by quantitative HSQC (/100 C9 unit)

45



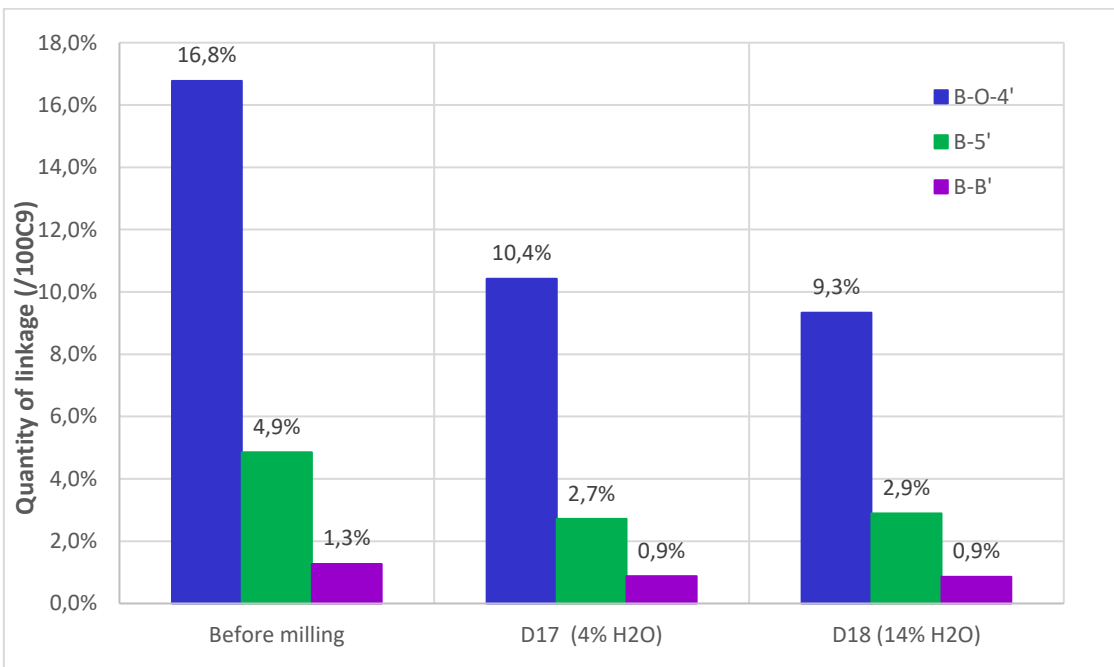




46 **Figure 6** – HSQC NMR Spectra of Purified Biolignin<sup>TM</sup> before milling (a); after 120  
 47 min milling without the presence of NaOH (C1, b), and with NaOH after 30 min milling  
 48 (D5, c), 60 min milling (D7, d), 120 min milling (D9, e)

49

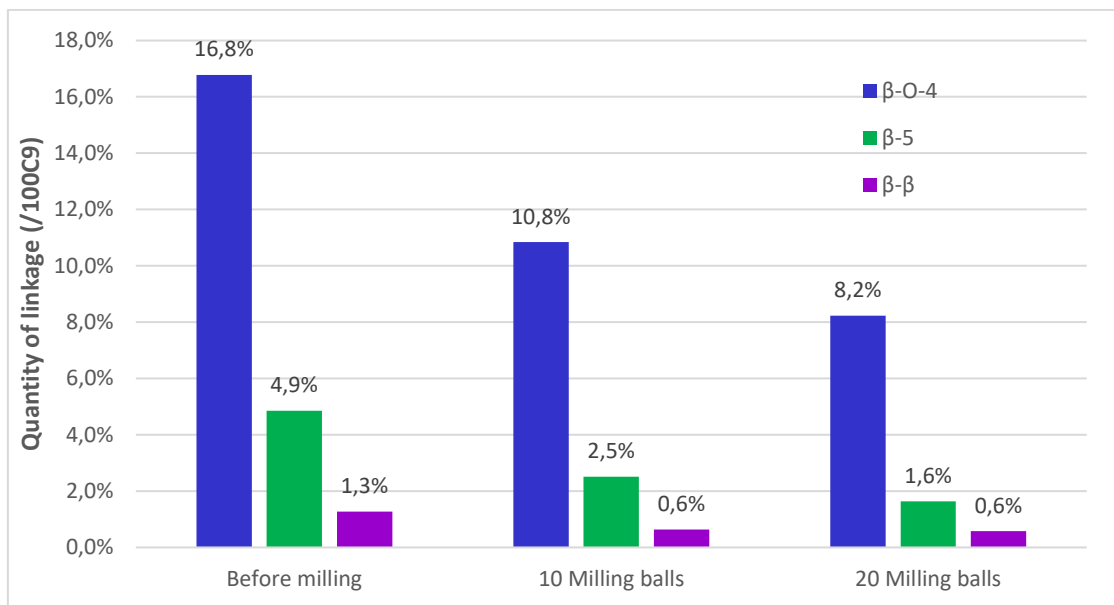
50



51

52 **Figure 7** - Occurrence of  $\beta$ -O-4',  $\beta$ -5' and  $\beta$ - $\beta'$  (/100 C9 unit) in Biolignin<sup>TM</sup>, D17 and  
 53 D18 as determined by quantitative NMR HSQC

54



55  
56  
57

**Figure 8** - Occurrence of  $\beta$ -O-4',  $\beta$ -5' and  $\beta$ - $\beta$ ' (/100 C9 unit) in Biolignin™, after milling with 10 balls and 20 balls as determined by quantitative NMR HSQC

1 **Mechanochemical cleavage of lignin in presence of sodium hydroxide**  
2 **to produce a homogeneous lignin fraction optimized for a direct use in**  
3 **applications**

4 Nadja Cachet<sup>1,3</sup>, Pierre Lavedan<sup>2</sup>, Michel Baltas<sup>3\*</sup>, Bouchra Benjelloun-Mlayah<sup>1\*</sup>

5

6 <sup>1</sup> CIMV, 109 rue Jean Bart, Diapason A, F-31670 Labège, France

7 <sup>2</sup> Institut de Chimie de Toulouse, UAR 2599, 118 Route de Narbonne, Toulouse Cedex  
8 09, 31062, France

9 <sup>3</sup> CNRS, LCC (Laboratoire de Chimie de Coordination), Université de Toulouse, UPS,  
10 205 Route de Narbonne, BP 44099, Cedex 4, 31077 Toulouse, France

11 \* Corresponding authors Email: michel.baltas@lcc-toulouse.fr; b.benjelloun@cimv.fr

12

13

14 **Table captions**

15 **Table 1.** Identification and quantification of the impurities within the Biolignin<sup>TM</sup>  
16 fraction

17 **Table 2.** Molecular profile of Biolignin<sup>TM</sup> determined by GPC

18 **Table 3.** Molecular weight distribution in Biolignin<sup>TM</sup> and fractions

19 **Table 4.** Identification and quantification of the impurities within the Biolignin<sup>TM</sup>  
20 fractions

21 **Table 5.** ATR-FT-IR of purified Biolignin<sup>TM</sup> and Biolignin<sup>TM</sup>

22 **Table 6.** <sup>31</sup>P NMR quantification of Biolignin<sup>TM</sup> and purified Biolignin<sup>TM</sup> using endo-  
23 N-hydroxy-5-norbornene-2,3-dicarboximide as an internal standard

24 **Table 7.** 6 main lignin moieties of Biolignin<sup>TM</sup> and Purified Biolignin<sup>TM</sup> quantified by  
25 HSQC

26 **Table 8.** Mechanochemical experiments tested on Purified Biolignin<sup>TM</sup> and their  
27 conditions

28 **Table 9.** Average relative molecular mass of milled samples as a function of its  
 29 moisture content, as determined by GPC

30 **Table 10.** Average relative molecular mass determined by GPC of milled samples with  
 31 or without the presence of methanol as a scavenger

32 **Table 11.** Average relative molecular mass of milled Biolignin™ samples as a function  
 33 of its moisture content, as determined by GPC

34 **Table 12.** <sup>31</sup>P NMR quantification of COOH and OH groups and Biolignin™, D17 and  
 35 D18

36 **Table 13.** Mechanochemical experiments on Biolignin™ tested, their conditions and  
 37 the average molecular mass of the final sample as determined by GPC

39 **Table 1** – Identification and quantification of the impurities within the Biolignin™  
 40 fraction

<b>Ashes content (% , Dry Matter)</b>		1.02
<b>Carbohydrates content</b>	<b>Glucose (% , DM)</b>	2.31
	<b>Xylose (% , DM)</b>	1.83
<b>Protein content (% , DM)</b>		7.80

41

42 **Table 2** – Molecular profile of Biolignin™ determined by GPC

<b>Mn (g/mol)</b>	999
<b>Mw (g/mol)</b>	1743
<b>P (M<sub>w</sub>/M<sub>n</sub>)</b>	1.8

43

44 **Table 3** – Molecular weight distribution in Biolignin™ and fractions

	<b>Solvent</b>	<b>Yield (%)</b>	<b>M<sub>n</sub> (g/mol)</b>	<b>M<sub>w</sub> (g/mol)</b>	<b>P (M<sub>w</sub>/M<sub>n</sub>)</b>
<b>F1</b>	Et <sub>2</sub> O	6.4 (±0.5)	611 (3.8 u*)	784 (4.8 u)	1.3
<b>F2</b>	CH <sub>2</sub> Cl <sub>2</sub>	16.2 (±1.2)	747 (4.6 u)	1116 (6.9 u)	1.5
<b>Purified Biolignin™</b>	MeOH	48.4 (±2.2)	983 (6.1 u)	1579 (9.7 u)	1.6
<b>Insoluble residue</b>	-	29.0 (±2.7)	<i>Highly insoluble but &gt; 1700 g/mol</i>		
<b>Biolignin™</b>	-	-	999 (6.2 u)	1743 (10.8 u)	1.8

\* u = C9-unit of wheat straw Biolignin™ (Lange et al. 2016)

45

46 **Table 4** - Identification and quantification of the impurities within the Biolignin™  
 47 fractions

	<b>Purified Biolignin™</b>	<b>Biolignin™</b>
<b>Ashes content (% , Dry Matter)</b>	0.44	1.02
<b>Hemicelluloses (% , DM)</b>	2.3	4.1
<b>Protein content (% , DM)</b>	6.2	7.8

Total (% DM)	8.94	12.92
--------------	------	-------

48

49

**Table 5** - ATR-FT-IR of purified Biolignin<sup>TM</sup> and Biolignin<sup>TM</sup>

Purified Biolignin <sup>TM</sup>	Biolignin <sup>TM</sup>	
3368	3377	O-H Stretch
2925	2936	C-H Stretch in CH <sub>3</sub> /or and CH <sub>2</sub> groups
2850	2855	C-H Stretch in O-CH <sub>3</sub> groups
1713	1714	C=O Stretch in unconjugated ketones, carboxyls and ester groups
1653	1654	Ring conjugated C=C Stretch of <b>Coniferyl/ Synapyl alcohol</b>
1599	1598	Aryl ring Stretching, symmetric
1509	1508	Aryl ring Stretching, asymmetric
1458	1456	C-H deformation asymmetric in CH <sub>3</sub> and CH <sub>2</sub>
1422	1425	Aromatic skeletal vibration combined with C-H in-plane deformation
1372	1363	C-H deformation asymmetric of O-CH <sub>3</sub> groups
1330	1330(sh)	<b>Syringyl ring</b> breathing with C-O stretch
1227	1222	C=C stretching of <b>Guaiacyl ring</b> , Phenolic OH, alkyl-aryl ether asymmetric C-O-C
1159	1160	Aromatic C-H in plane deformation, typical of <b>Guaiacyl units</b>
1140	1140	Aromatic C-H in-plane deformation; typical of <b>Guaiacyl units</b> ; whereby G Condensed > etherified (typical for S units); C-O Stretching
1118	1118	Aromatic C-H in plane deformation, typical of <b>Syringyl units</b> , secondary alcohols
1029	1029	Aromatic C-H in plane deformation of <b>Guaiacyl units</b> , C-O deformation in primary alcohols
869	869	C-H deformation out of plane, Aromatic ring
839	835	C-H deformation out of plane in position 2 and 6 of <b>Syringyl and in all p-Hydroxyphenyl units</b>

50 \* sh: Shoulder

51

**Table 6** – <sup>31</sup>P NMR quantification of Biolignin<sup>TM</sup> and purified Biolignin<sup>TM</sup> using endo-N-hydroxy-5-norbornene-2,3-dicarboximide as an internal standard

Quantification (mmol/g)	Biolignin <sup>TM</sup>	Purified Biolignin <sup>TM</sup>
-COOH	0.76	0.65
H-units phenolic -OH	0.39	0.39
G-units phenolic -OH	0.83	0.74
S-units and condensed G-units phenolic -OH	1.09	0.93
Aliphatic - OH	2.05	2.00
<b>Total -OH (mmol/g)</b>	<b>4.36</b>	<b>4.06</b>
Total Alk-OH (mmol/g)	2.05	2.00
Total Ar-OH (mmol/g)	2.31	2.06

54

**Table 7** – 6 main lignin moieties of Biolignin<sup>TM</sup> and Purified Biolignin<sup>TM</sup> quantified by HSQC

Name	Ref. signal	Biolignin <sup>TM</sup>	Purified Biolignin <sup>TM</sup>
Arylglycerol- $\beta$ -arylether ( $\beta$ -O-4') substructure (1)	C <sub><math>\alpha</math></sub> H (ref)	69.7%	73.6%
Phenylcoumaran ( $\beta$ -5') substructure (2)	C <sub><math>\alpha</math></sub> H	15.4%	10.7%
Resinol ( $\beta$ - $\beta'$ ) substructure (3)	C <sub><math>\beta</math></sub> H	7.6%	5.1%
1,2-diarylpropane ( $\beta$ -1') substructure (4)	C <sub><math>\alpha</math></sub> H	0.4%	1.1%
Monotetrahydrofuran ( $\alpha$ -O- $\alpha'$ and $\beta$ - $\beta'$ ) substructure (5)	C <sub><math>\alpha</math></sub> H	3.8%	3.1%

$\alpha,\beta$ -diarylether ( $\alpha$ -O-4' and $\beta$ -O-4'') substructure (6)	C <sub>6</sub> H	3.2%	6.7%
---	------------------	------	------

57  
58  
59

**Table 8** – Mechanochemical experiments tested on Purified Biolignin<sup>TM</sup> and their conditions

	Purified Biolignin <sup>TM</sup> (mg)	NaOH (mg)	H <sub>2</sub> O ( $\mu$ L)	MeOH ( $\mu$ L)	Reaction time (min)	wt% H <sub>2</sub> O	$\eta^*$	
C1	700	0	0	0	120	4%	0.03	
Optimization of reaction time	D1	350	350	0	15	4%	0.03	
	D2	350	350	0	30	4%	0.03	
	D3	350	350	0	60	4%	0.03	
	D4	350	350	0	120	4%	0.03	
Optimization of quantity of NaOH	D5	650	160.5	0	30	4%	0.03	
	D6	650	321	0	30	4%	0.03	
	D7	650	160.5	0	60	4%	0.03	
	D8	650	321	0	60	4%	0.03	
	D9	650	160.5	0	120	4%	0.03	
	D10	650	321	0	120	4%	0.03	
H <sub>2</sub> O effect	D11	650	160.5	41.6	-	60	10%	0.08
	D12	650	160.5	72.1	-	60	14%	0.11
	D13	650	160.5	105.9	-	60	18%	0.14
	D14	650	160.5	141.2	-	60	24%	0.22
MeOH effect	D15	650	160.5	-	175.5	30	4%	0.22
	D16	650	160.5	-	175.5	60	4%	0.22

60 \* $\eta$ : empiric parameter which determine if the reaction respect the Liquid-assisted Grinding (LAG)  
61 condition (*i.e.*  $0 < \eta < 2 \mu\text{L}/\text{mg}$ ).  $\eta = V$  (liquid;  $\mu\text{L}$ )/ $m$  (solid reagents; mg) (Ying et al. 2021)  
62

63 **Table 9** – Average relative molecular mass of milled samples as a function of its  
64 moisture content, as determined by GPC

	wt% H <sub>2</sub> O	M <sub>n</sub> (g/mol)	M <sub>w</sub> (g/mol)
Purified Biolignin <sup>TM</sup>	4%	983 (6.1 u)	1579 (9.7 u)
D7	4%	797 (4.9 u)	1143 (7.1 u)
D11	10%	720 (4.4 u)	1038 (6.4 u)
D12	14%	688 (4.2 u)	1028 (6.3 u)
D13	18%	617 (3.8 u)	911 (5.6 u)
D14	24%	855 (5.3 u)	1167 (7.2 u)

\* u = C9-unit of wheat straw Biolignin<sup>TM</sup> (Lange et al. 2016)

65  
66  
67

**Table 10** - Average relative molecular mass determined by GPC of milled samples with or without the presence of methanol as a scavenger

	wt% H <sub>2</sub> O	MeOH	Milling time (min)	M <sub>n</sub> (g/mol)	M <sub>w</sub> (g/mol)
Purified Biolignin <sup>TM</sup>	4%	-	-	983 (6.1 u)	1579 (9.7 u)

D5	4%	-	30	901 (5.5 u)	1201 (7.4 u)
D7	4%	-	60	797 (4.9 u)	1143 (7.1 u)
D13	18%	-	60	617 (3.8 u)	911 (5.6 u)
D15	4%	Yes	30	638 (3.9 u)	988 (6.1 u)
D16	4%	Yes	60	645 (4.0 u)	1010 (6.2 u)

\* u = C9-unit of wheat straw Biolignin<sup>TM</sup> (Lange et al. 2016)

68

69 **Table 11** – Average relative molecular mass of milled Biolignin<sup>TM</sup> samples as a  
70 function of its moisture content, as determined by GPC

	Biolignin <sup>TM</sup> (mg)	NaOH (mg)	H <sub>2</sub> O (μL)	Reaction time (min)	wt% H <sub>2</sub> O	η	M <sub>n</sub> (g/mol)	M <sub>w</sub> (g/mol)
<b>Biolignin<sup>TM</sup></b>	-	-	-	-	<b>4%</b>		999 (6.2 u)	1743 (10.8 u)
<b>C2</b>	700	0	0	60	4%	0.03	978 (6.0 u)	1662 (10.3 u)
<b>D17</b>	650	160.5	0	60	4%	0.03	607 (3.8 u)	1015 (6.3 u)
<b>D18</b>	650	160.5	72.2	60	14%	0.11	591 (3.7 u)	903 (5.6 u)
<b>D19</b>	650	160.5	105.8	60	18%	0.14	-	-

\* u = C9-unit of wheat straw Biolignin<sup>TM</sup> (Lange et al. 2016)

71

72 **Table 12** – <sup>31</sup>P NMR quantification of COOH and OH groups and Biolignin<sup>TM</sup>,  
73 D17 and D18

Quantification (mmol/g of sample)	Biolignin <sup>TM</sup>	D17	D18
-COOH	0.76	1.03	1.04
Phenolic - OH of H-unit	0.39	0.32	0.31
Phenolic - OH of G-unit	0.83	0.76	0.79
Phenolic - OH of S-unit	0.52	0.48	0.51
5-5' condensed unit	0.25	0.22	0.24
4-O-5' condensed unit	<b>0.46</b>	<b>0.08</b>	<b>0.07</b>
Aliphatic - OH	2.05	1.95	1.87

74

75

76 **Table 13** - Mechanochemical experiments on Biolignin<sup>TM</sup> tested, their conditions and  
77 the average molecular mass of the final sample as determined by GPC

	Biolignin <sup>TM</sup> (g)	NaOH (g)	Number of balls	Reaction time (min)	wt% H <sub>2</sub> O	η	M <sub>n</sub> (g/mol)	M <sub>w</sub> (g/mol)
<b>D20</b>	17.000	4.197	10	60	4%	0.03	592 (3.6 u)	939 (5.8)
<b>D21</b>	17.000	4.197	20	60	4%	0.03	484 (3.0 u)	772 (4.8 u)

78

79